Hydrol. Earth Syst. Sci., 19, 2427–2449, 2015
www.hydrol-earth-syst-sci.net/19/2427/2015/
doi:10.5194/hess-19-2427-2015

Hydrology and Earth System Sciences
Open Access

Assessing the simple dynamical systems approach in a Mediterranean context: application to the Ardèche catchment (France)

M. Adamovic[1,4], I. Braud[1], F. Branger[1], and J. W. Kirchner[2,3]

[1]Irstea, UR HHLY, Hydrology-Hydraulics Research Unit, Lyon-Villeurbanne, France
[2]Department of Environmental Systems Science, Swiss Federal Institute of Technology, ETH Zurich, Zurich, Switzerland
[3]Swiss Federal Research Institute WSL, Birmensdorf, Switzerland
[4]CNRS, HydroSciences Laboratory, Place Eugene Bataillon, 34095 Montpellier, France

Correspondence to: M. Adamovic (marko.adamovic@hotmail.com)

Received: 2 September 2014 – Published in Hydrol. Earth Syst. Sci. Discuss.: 24 September 2014
Revised: 27 March 2015 – Accepted: 25 April 2015 – Published: 22 May 2015

Abstract. This study explores how catchment heterogeneity and variability can be summarized in simplified models, representing the dominant hydrological processes. It focuses on Mediterranean catchments, characterized by heterogeneous geology, pedology and land use, as well as steep topography and a rainfall regime in which summer droughts contrast with high-rainfall periods in autumn. The Ardèche catchment (Southeast France), typical of this environment, is chosen to explore the following questions: (1) can such a Mediterranean catchment be adequately characterized by a simple dynamical systems approach and what are the limits of the method under such conditions? (2) what information about dominant predictors of hydrological variability can be retrieved from this analysis in such catchments?

In this work we apply the data-driven approach of Kirchner (2009) to estimate discharge sensitivity functions that summarize the behaviour of four sub-catchments of the Ardèche, using low-vegetation periods (November–March) from 9 years of measurements (2000–2008) from operational networks. The relevance of the inferred sensitivity function is assessed through hydrograph simulations, and through estimating precipitation rates from discharge fluctuations. We find that the discharge sensitivity function is downward-curving in double-logarithmic space, thus allowing further simulation of discharge and non-divergence of the model, only during low-vegetation periods. The analysis is complemented by a Monte Carlo sensitivity analysis showing how the parameters summarizing the discharge sensitivity function impact the simulated hydrographs. The resulting discharge simulation results are good for granite catchments, which are likely to be characterized by shallow subsurface flow at the interface between soil and bedrock. The simple dynamical system hypothesis works especially well in wet conditions (peaks and recessions are well modelled). On the other hand, poor model performance is associated with summer and dry periods when evapotranspiration is high and low-flow discharge observations are inaccurate. In the Ardèche catchment, inferred precipitation rates agree well in timing and amount with observed gauging stations and SAFRAN climatic data reanalysis during the low-vegetation periods. The model should further be improved to include a more accurate representation of actual evapotranspiration, but provides a satisfying summary of the catchment functioning during wet and winter periods.

1 Introduction

Catchments show a high degree of heterogeneity and variability, both in space and time (McDonnell et al., 2007) raising questions about the degree of complexity that must be used to model their behaviour (Sivapalan, 2003a). Many hydrological models are based on the bottom-up or reductionist approach (Sivapalan, 2003b; Zehe et al., 2006), following the blueprint proposed by Freeze and Harlan (1969). Governing equations such as the Darcy or Richards' equation, which are inherent in many hydrological models, are

suitable for point-scale processes (Bloschl and Sivapalan, 1995; Kirchner, 2006). Their use to describe processes at larger scales leads to the calibration of "effective parameters" which are sometimes difficult to link with measurable quantities (Sivapalan, 2003b), although recent methods combining the use of small-scale variability and regionalization techniques were shown to be efficient in preserving spatial patterns of variability (Samaniego et al., 2010). Such "effective" large-scale equations might not, however, describe hydrologic processes realistically, even if they can be calibrated to reproduce observed catchment behaviour (Kirchner, 2006). Klemeš (1983) was one of the first hydrologists proposing the use of alternative modelling concepts. He defines the top-down or downward approach as the "route that starts with trying to find a distinct conceptual node directly at the level of interest (or higher) and then looks for the steps that could have led to it from a lower level". To go in this direction, Sivapalan (2003b) and Kirchner (2006) promote a combination of data analysis and process conceptualization (the top-down approach). This allows understanding of the main drivers of the system functioning (the perceptual model; Beven, 2002) and inferring the system's "emergent properties" (Sivapalan, 2003b) or "functional traits" (McDonnell et al., 2007). Thus, models obtained through this approach are simple, with a limited number of parameters that can be estimated from the available data.

Kirchner (2009) represents a catchment with a simple bucket model in which system parameters are derived directly from measured streamflow fluctuations during recession periods. He based his analysis on storage–discharge relationships with one essential assumption: discharge depends only on the total water stored in the catchment. This approach allows the derivation of a first-order nonlinear differential equation for simulating rainfall–runoff behaviour. Until now, this approach has mostly been applied in small, humid catchments. Kirchner (2009) obtained good results for the Severn (8.70 km^2) and Wye (10.55 km^2) catchments at Plynlimon, in Mid-Wales. Teuling et al. (2010) also applied this approach to the Prealpine Rietholzbach catchment (3.31 km^2) getting good results in wet periods and poor model performance during dry periods. The study of Brauer et al. (2013) showed similar results for the Dutch lowland Hupsel Brook catchment (6.5 km^2) where discharge results were correctly reproduced only in certain periods. Melsen et al. (2014) determined the minimum amount of data required to find robust parameter values for a simple Kirchner (2009) model with two parameters in the Prealpine Rietholzbach catchment (3.31 km^2). They concluded that a two-parameter model is reasonably able to capture high flows but fails to describe the low flows.

Krier et al. (2012) applied the concept of doing hydrology backwards to infer spatially distributed rainfall rates in the Alzette catchment (1092 km^2) in Luxembourg, and found that introducing a soil moisture threshold led to model improvement, especially under the wet conditions. However, they did not simulate hydrographs. In addition, all those studies used data from well-monitored experimental catchments, and the method has not previously been applied using data from operational networks, which are much more common.

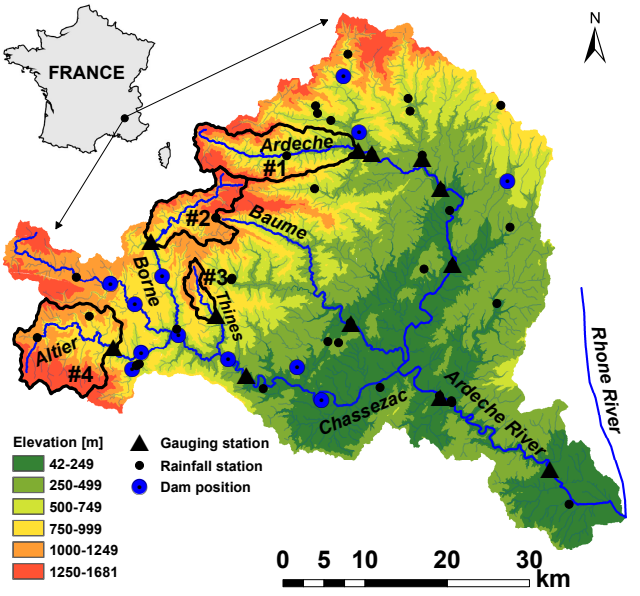

Figure 1. Map of the Ardèche catchment with gauging and rainfall stations, dam locations, and catchments that were examined: #1. Ardèche at Meyras; #2. Borne at Nicolaud Bridge; #3. Thines at Gournier Bridge; #4. Altier at Goulette.

To our knowledge, the simple dynamical system approach (SDSA) proposed by Kirchner (2009) has not been evaluated in a Mediterranean context, where the rainfall regime exhibits strong contrasts between dry conditions in summer and intense rainfall events, often related to stationary Mesoscale Convective Systems (Hernández et al., 1998), during autumns. Wittenberg and Sivapalan (1999), for instance, used recession analyses to estimate groundwater recharge in a Mediterranean type of climate in Australia, but they did not consider the storage–discharge relationship in its implicit differential form, the sensitivity function $g(Q)$.

Mediterranean catchments are also characterized by heterogeneous topography, vegetation and geology. The study of the water cycle in such Mediterranean conditions, as well as a better understanding and modelling of processes triggering flash floods, are central research topics addressed in the HyMeX (Hydrological Cycle in the Mediterranean Experiment; Drobinski et al., 2013) program[1] and in the FloodScale project (Braud et al., 2014)[2] to which this study contributes.

Our study area is the Ardèche catchment (2388 km^2, see location in Fig. 1), which is typical of Mediterranean catchments with highly variable rainfall, steep slopes, and heterogeneous geology and pedology. It is one of the studied

[1] www.hymex.org.

[2] http://floodscale.irstea.fr/.

catchments of the Cévennes–Vivarais Hydro-Meteorological Observatory (OHM-CV, Boudevillain et al., 2011). Previous studies in this catchment mainly focused on flood forecasting and discharge quantile estimation. Discharge time series from the Ardèche catchment were used to assess the value of new observations in estimating extreme quantiles, such as information derived from palaeofloods (Sheffer et al., 2002), historical floods (Lang et al., 2002; Naulet et al., 2005) or post-flood survey peak discharge estimates (Gaume et al., 2009). Flood forecasting studies extended to the whole Cévennes–Vivarais region are numerous and include work by Sempere-Torres et al. (1992), Duband et al. (1993), Le Lay and Saulnier (2007), Saulnier and Le Lay (2009), Tramblay et al. (2010) and Garambois et al. (2013). Use of distributed hydrological models for process understanding during flash floods in the Cévennes–Vivarais region is more recent. Examples of such studies are those of Bonnifait et al. (2009), Manus et al. (2009), and Braud et al. (2010). Those studies use a reductionist approach to gain insight into active hydrological processes during floods and highlight a lack of data or parameter information.

As a complementary approach to the modelling studies mentioned above, we adopt in this study the data-based approach proposed by Kirchner (2009) to estimate the hydrological water balance of the Ardèche catchment and to gain insight into the dominant associated processes. Like in the work of Melsen et al. (2014), we divided our examined period into vegetation period (April–October) and low-vegetation period (November–March) where evapotranspiration can be considered as a low.

The idea is to use this insight to propose simple models with very few parameters to learn more about hydrological functioning at the catchment scale.

In the present paper, we focus on the following questions: (1) what is the applicability of the simple dynamical systems approach (SDSA) and what are its limitations in a Mediterranean type catchment like the Ardèche with its particular conditions (size, climate, geological and pedological heterogeneity), and when data from operational networks are used? (2) what can we learn about dominant hydrological processes using this methodology?

To answer those questions, we first estimate the discharge sensitivity function using the available discharge data. Then we assess the relevance of the obtained function by testing how well the simple model based on it can simulate observed discharge, and can retrieve rainfall. The study is complemented by examining the sensitivity of the results to the parameters of the discharge sensitivity function.

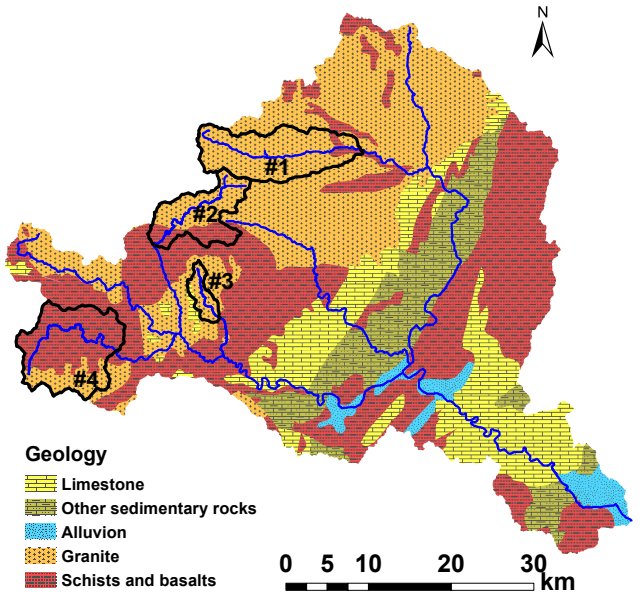

Figure 2. Geological map of the Ardèche catchment (extracted and processed from geological map of France 1 : 1 000 000 issued by BRGM (6th edition, 1996).

2 Field site and data

2.1 The Ardèche catchment

The Ardèche catchment is located in southern France (Fig. 1). The catchment has an area of 2388 km^2, and the Ardèche River itself has a length of 125 km. There are two main tributaries in the Ardèche Basin: the Baume and Chassezac rivers, which join the Ardèche River close to one another. Elevation ranges from the mountains of the Massif Central (highest point: 1681 m) in the northwest, to the confluence with the Rhone River (lowest point: 42 m) in the southeast.

The main lithologies found in the Ardèche are schist, granite, and limestone (Fig. 2). Upstream, the Ardèche flows from west to east in a deep granite valley, then flows through basalt formations and schist in a north–south direction. Downstream, it flows through bedded and massive limestone before flowing into the Rhone River (see for example the description provided by Naulet et al., 2005).

Among the land use types found in the Ardèche, forest dominates throughout the basin (Corine Land Cover database[3]). Forest is represented by a mix of coniferous (27 %), broadleaf (13 %) and Mediterranean trees (17 %). Shrubs and bushes are also well represented in the catchment, occupying a significant portion of the area (17 %). We also distinguish significant areas of bare soil in the central and southern part of the Ardèche, as well as a few small urban areas and areas of early and late crops.

[3]http://sd1878-2.sivit.org/

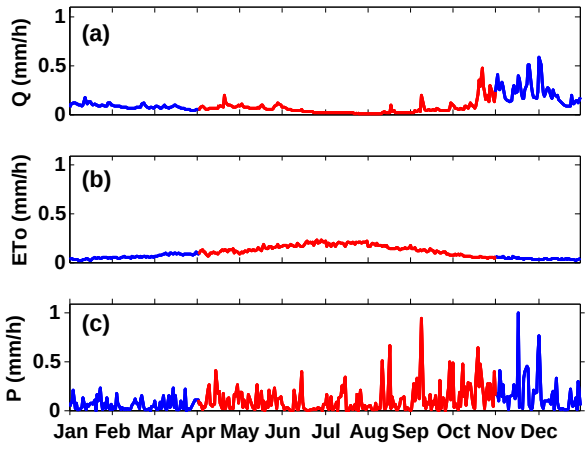

Figure 3. Average hourly discharge **(a)**, reference ET_0 **(b)** and rainfall **(c)** in (mm h^{-1}) at the Ardèche outlet for all months between 2000 and 2008. **(b)** and **(c)** are calculated from the SAFRAN reanalysis. In red: vegetation period; in blue: low-vegetation period.

In the Ardèche Basin, there is a strong influence of the Mediterranean climate with seasonally heavy rainfall events during autumn. Historical data show that these events usually lead to flash floods: Lang et al. (2002) mention seven rainfall events locally exceeding 400 mm during the 1961–1996 period. They also comment on the relatively quick flow response (a couple of hours) to precipitation due to the steepness of the upstream part of the catchment and presence of granitic and basaltic rocks.

Figure 3 shows the average hourly regime of the main terms of the water balance equation for all months between 2000 and 2008, differently coloured with respect to vegetation (red) and low-vegetation periods (blue). Under the main terms of the water balance we consider discharge, evapotranspiration and precipitation. As we consider interannual values, change in water storage is assumed to be zero. This hypothesis is consistent with the lack of a regional aquifer in the Ardèche catchment. The hydrological year consists mainly of two periods. There is a rainy season (September–February) with maximum precipitation intensity in autumn, characterized by rainfall amounts greatly exceeding reference evapotranspiration ET_0 (calculated based on the SAFRAN reanalysis of Quintana-Seguí et al., 2008: see next section), and by high discharge. On the other hand, during the dry season (March–August), on average ET_0 is much larger than precipitation and runoff is low. Evapotranspiration is influenced by the seasonal cycles of temperature, radiation and vegetation, the latter being particularly marked in the Ardèche catchment, which is mostly covered by forests (around 60 % of the total catchment area, with 27 % of the forest being coniferous and thus remaining green even in winter).

2.2 Available data and first data consistency analysis

2.2.1 Observations used in the study

In the Ardèche catchment, measurements of the hydrological state variables were mainly started in the 1960s for the purpose of flood forecasting. In our study, we use hourly data of precipitation (P), reference evapotranspiration (ET_0) and discharge (Q) from the period 1 January 2000 until 31 December 2008. These data come from operational networks, and not from research catchments as in previous applications of the SDSA, which renders the study challenging and interesting, as operational networks account for a large fraction of the available discharge data in many regions.

The analysis is mostly constrained by the availability of discharge data, which were obtained from the national Banque Hydro website (www.hydro.eaufrance.fr) and Electricité de France (france.edf.com/). Unfortunately, numerous dams and hydro-power stations are located in the upper parts of the Ardèche and Chassezac catchments (Fig. 1). These dams are used to regulate the water level throughout the year, in particular to ensure a sufficient discharge in the river for recreational use in the summer period. Data to reconstruct natural discharge at the hourly time step were not available. Thus we had to discard several gauging stations located downstream of the dams in order to apply the simple dynamical system approach to data where the water balance can be closed.

As the stations were not designed and managed for low-flow measurements, the low-flow time series were investigated by contacting the operational services in charge of the stations. Consequently, two stations had to be removed from further analysis due to unreliable measurements and agriculture water withdrawals in summer periods. Ultimately, four sub-catchments could be examined: the Ardèche at Meyras (#1), the Borne at Nicolaud Bridge (#2), the Thines at Gournier Bridge (#3), and the Altier at Goulette (#4); see locations in Fig. 1. These four sub-catchments are characterized by steep slopes (> 15 %), average altitude of around 1000 m and igneous and metamorphic bedrock. We have also computed Strahler stream order and channel length using TauDEM tools (Tarboton et al., 2009) in order to classify and measure the size of the river network. The analysis was conducted using the 25 m resolution IGN DTM and the D8 flow direction algorithm, so the resulting network statistics may only loosely resemble those that would be obtained from more accurate procedures such as field mapping. Main physiographic catchment characteristics are summarized in Table 1.

The discharge data were available at varying time intervals, and were aggregated to hourly sums. Two types of precipitation data have been examined and are used throughout the analysis. Local rain gauges at the hourly time step provided by the OHM-CV database (Boudevillain et al., 2011) are used as the primary source of rainfall data for the catch-

Table 1. Physiographic characteristics of the four examined Ardèche sub-catchments. Strahler stream order, channel length and drainage density are calculated from the 25 m IGN DTM using TauDEM tools (Tarboton et al., 2009).

Catchment ID River and catchment name	#1 Ardèche at Meyras	#2 Borne at Nicolaud Bridge	#3 Thines at Gournier Bridge	#4 Altier at Goulette
River name	Ardèche	Borne	Thines	Altier
Drainage area (km^2), A	98.43	62.6	16.73	103.42
Average altitude (m)	898.54	1113	892.75	1149.13
Average slope (%)	23.43	20.13	16.72	17.13
Forest cover (%)	68	68	51	42
Strahler stream order	4	3	3	5
Channel length (km), L	94.31	59.26	13.51	97.38
Drainage density ($km\,km^{-2}$), $D = L/A$	0.96	0.95	0.81	0.94

ment Ardèche at Meyras (#1). For the catchments Borne at Nicolaud Bridge (#2), Thines at Gournier Bridge (#3) and Altier at Goulette (#4) we use the SAFRAN reanalysis of Météo-France, based on 8 by 8 km^2 grids (Quintana-Seguí et al., 2008; Vidal et al., 2010) since either the local rain gauge shows lack of data and time gaps, or there is no rain gauging station in the catchment (e.g. Thines at Gournier Bridge (#3). These precipitation data are calculated as catchment averages at hourly time steps. To compute the reference evapotranspiration ET_0, we also used the climate variables of the SAFRAN reanalysis of Météo-France at an hourly time step. ET_0 is calculated using the Penman–Monteith formula according to FAO recommendations (Allen et al., 1998). In order to account for vegetation type, we compute potential evapotranspiration (PET) as reference evapotranspiration ET_0 modulated by a crop coefficient depending on the nature of vegetation for each catchment (Eq. 1).

$$\mathrm{PET} = K_\mathrm{C} \cdot \mathrm{ET}_0 \tag{1}$$

We also took into account the seasonal variability of vegetation through the definition of three crop coefficient stages: initial (1 January–1 April), mid-season (15 April–15 October) and late season (1 November–31 December). Periods between initial and mid-season as well as between mid-season and late season are interpolated linearly. The values of crop coefficients for the Ardèche catchments were obtained through the FAO database (Allen et al., 1998). For each catchment we determined the cover estimates for each vegetation type (Broad-leaf forest, Mediterranean forest, Coniferous forest, Early crops, Late crops, Shrubs and bushes and Bare soil) and we calculated a weighted average crop coefficient per sub-catchment for each stage (see Table 2). Reference evapotranspiration ET_0 and ET_0 modulated by the crop coefficient ($K_\mathrm{C}ET_0$) over the examined period (2000–2008) are given in Table 3.

2.2.2 Data consistency

To further assess data quality, we evaluated the consistency of the local rainfall station with SAFRAN data for the Ardèche at Meyras (#1) catchment at the hourly time step. The resulting coefficient of determination was 0.99. For the rest of the sub-catchments, we first assumed that SAFRAN rainfall is representative of the catchment average. However, by looking at the mean annual water fluxes (Table 3) and estimated runoff coefficients, we infer that the mass balances for catchments #2, #3 and # 4 are implausible.

For these reasons, two actual evapotranspiration (AET) estimates and runoff coefficients are provided to gain useful insight about data uncertainty. In Table 3 the first evapotranspiration estimate comes from the water balance $\mathrm{AET_{WB}} = P - Q$, where P is the average annual precipitation and Q the annual runoff, assuming that change in water storage is null. In Table 3, the first runoff coefficient (C) is calculated as the ratio between Q and P. We also note that $\mathrm{AET_{WB}}$ shows either high underestimation (#2 and #4) or overestimation (#3) in comparison with the $K_\mathrm{C}ET_0$ data, which once again points out the water balance closure issue.

In Table 4 the second AET estimate corresponds to Turc (1951) annual actual evapotranspiration, which is calculated using the following formula:

$$\mathrm{AET_{Turc}} = \frac{P}{\sqrt{0.9 + \frac{P^2}{L^2}}}, \tag{2}$$

where P is annual precipitation in $mm\,yr^{-1}$ and $L = 300 + 25\,T + 0.05\,T^3$ (T is the average annual temperature in °C). Here, the second runoff coefficient (C_Turc) is calculated using the following equation:

$$C_\mathrm{Turc} = \frac{P - \mathrm{AET_{Turc}}}{P}, \tag{3}$$

where C_Turc is the runoff coefficient, P is precipitation ($mm\,yr^{-1}$) and $\mathrm{AET_{Turc}}$ is the actual Turc evapotranspiration

Table 2. Weighted average crop coefficient for each examined catchment per growing stage.

Catchment name	K_c_initial (Jan–Apr)	K_c_mid_season (May–Oct)	K_c_late_season (Nov–Dec)
The Ardèche at Meyras (#1)	0.74	0.94	0.79
Borne at Nicolaud Bridge (#2)	0.73	0.96	0.80
Thines at Gournier Bridge (#3)	0.68	0.94	0.75
Altier at Goulette (#4)	0.62	0.97	0.75

Table 3. Hydro-climatic characteristics of the four examined Ardèche sub-catchments (2000–2008).

Catchment ID	#1	#2	#3	#4
Catchment name	Ardèche at Meyras	Borne at Nicolaud Bridge	Thines at Gournier Bridge	Altier at Goulette
Precipitation (mm yr^{-1}), P	1621	1633	1892	1176
Streamflow (mm yr^{-1}), Q	1057	1579	970	932
Runoff coefficient, C	0.65	0.97	0.51	0.79
Actual evapotranspiration (mm yr^{-1}), $AET_{wb} = P - Q$	564	54	922	244
ET_0 SAFRAN (mm yr^{-1})	809	792	860	775
K_c ET_0 (mm yr^{-1})	731	729	762	699

(mm yr^{-1}). We use AET_{Turc} in this formula along with precipitation in order to estimate annual runoff coefficients in the examined catchments.

The values of the water balance components differ from catchment to catchment as illustrated in Table 3. By comparing Tables 3 and 4, we note that the mass balance AET_{WB} and AET_{Turc} estimates are only consistent for the Ardèche at Meyras (#1) catchment; at the other three sites they differ greatly, leading to inconsistent runoff coefficients for the same catchment. This suggests that either the rainfall or ET_0 (or possibly both) are not representative at the other catchments. Regarding rainfall, the gridded SAFRAN product is known to underestimate precipitation in mountainous areas and to underestimate the occurrence of strong precipitation, which could help to explain the water balance closure problems (see Sect. 5.1 for more details).

Discharge data uncertainty has been addressed in many works and sometimes it can be quite large, especially in catchments where high flows are seldom gauged due to safety reasons (Le Coz et al., 2010) or where low flows may be difficult to measure accurately. Nevertheless, here we decided to go ahead with the available operational discharge data, to assess whether the SDSA can provide useful information about catchment hydrological functioning in a Mediterranean context, even in the presence of some uncertainty in the discharge data.

However, in order to apply the SDSA with data where water balance closure is more representative, we rescaled precipitation and K_cET_0 values for catchments (#2, #3 and #4). Our rescaling scheme (see next section for more details) assumes that the discharge data were accurate enough for the application of the SDSA, which relies mainly on discharge data.

2.3 Rescaling of water balance fluxes

The first step in the rescaling analysis was to obtain a robust estimate of actual evapotranspiration.

We used the following equation of Fu (1981) to draw Budyko (1974) type curves for the Ardèche catchments:

$$\frac{AET}{P} = 1 + \frac{ET_0}{P} - \left[1 + \left(\frac{ET_0}{P}\right)^w\right]^{\frac{1}{w}}, \quad (4)$$

where AET / P is the evapotranspiration ratio, ET_0/P is the dryness index and w is a catchment parameter.

The parameter w was empirically derived by Fu (1981) and it can have values from $1\sim$ to ∞. Zhang et al. (2004) defined parameter w as a coefficient representing "the integrated effects of catchment characteristics such as vegetation cover, soil properties and catchment topography on the water balance".

In our study, we drew Fu curves with parameter w ranging between 1.5 and 5 to gain insight about evapotranspiration ratios in the Ardèche. The next step was to compare those curves with mean actual annual evapotranspiration ratios obtained using the Turc (1951), Schreiber (1904), Pike (1964) and Budyko formulae (see Table 5). We note from Fig. 4 that almost all calculated AET/P ratios lie in a w range between 1.7 and 3. On the other hand, the AET estimates derived using $AET_{WB} = P - Q$ (cyan colour in Fig. 4) for catchments #2, #3 and #4 were found to lie outside the range of values given by the various formulae, highlighting the water balance problem. Finally, to assess and adjust our data sets (P

Table 4. Scaling hydro-climatic characteristics of the four examined Ardèche sub-catchments (2000–2008).

Catchment ID Catchment name	#1 Ardèche at Meyras	#2 Borne at Nicolaud Bridge	#3 Thines at Gournier Bridge	#4 Altier at Goulette
Turc actual evapotranspiration ($\mathrm{mm\,yr^{-1}}$), $\mathrm{AET_{Turc}}$	609	505	571	475
Runoff coefficient, C_{Turc}	0.62	0.69	0.70	0.60
Temperature (°C), T	11.2	8.0	9.9	7.7
P_{Turc} ($\mathrm{mm\,yr^{-1}}$)	–	2084	1541	1407
Scaling P coefficient, α_P	–	1.27	0.81	1.2
Scaling AET coefficient, α_{AET}	–	0.69	0.75	0.68
New runoff coefficient, C_n	0.65	0.76	0.63	0.66

Table 5. Description of different empirical formulas for estimating mean annual actual evapotranspiration: AET is actual evapotranspiration ($\mathrm{mm\,yr^{-1}}$), P is precipitation ($\mathrm{mm\,yr^{-1}}$), $\mathrm{ET_0}$ is potential evapotranspiration ($\mathrm{mm\,yr^{-1}}$), and T is mean air temperature (°C).

Equation	Reference
$\mathrm{AET} = P[1-\exp\left(-\frac{\mathrm{ET_0}}{P}\right)]$	Schreiber (1904)
$\mathrm{AET} = \frac{P}{\sqrt{0.9+\left(\frac{P}{L}\right)^2}}$ where $L = 300+25T+0.05T^3$	Turc (1951)
$\mathrm{AET} = P/\left[1+\left(\frac{P}{\mathrm{ET_0}}\right)^2\right]^{0.5}$	Pike (1964)
$\mathrm{AET} = \left[P\left(1-\exp\left(-\frac{\mathrm{ET_0}}{P}\right)\right)\mathrm{ET_0}\tanh\left(\frac{P}{\mathrm{ET_0}}\right)\right]^{0.5}$	Budyko (1974)

and AET), we chose Turc-inferred evapotranspiration as representative for future analysis. In the 1951 paper, Turc reports an evaluation of his formula by comparing measured interannual discharge to values estimated through $P-\mathrm{AET}$ where AET is estimated by Eq. (2) of the paper with generally good performance. The considered data set covered countries all over the world. Thus, relying only on the P and T and not on $\mathrm{ET_0}$, we could avoid the use of evapotranspiration and reduce uncertainty in estimating AET. In addition, the Turc equation is widely used in France to estimate AET, and thus our results can be compared to other studies.

We then make the following assumptions. We assume that the long-term average Q is valid. We also assume that the "relative" day-to-day variations of $K_{\mathrm{c}}\ \mathrm{ET_0}$ and P are valid, but that the mean P does not reflect the whole-catchment P, and the mean $K_{\mathrm{c}}\mathrm{ET_0}$ does not reflect the mean AET. Therefore the means need to be rescaled to achieve a consistent set of measurements. As mentioned before, we assume that the Turc (1951) formula correctly describes the relationship between average AET and average P. Then we iteratively solve the Turc formula to find long-term average $\mathrm{AET_{Turc}}$ and P_{Turc} that are consistent with one another, and consistent with the average Q.

The hourly precipitation values are then rescaled by multiplying them by the ratio found in the previous step between the average P_{Turc} and the average measured P. Secondly, the $\mathrm{ET_0}$ values are also rescaled by multiplying the hourly $K_c\mathrm{ET_0}$ by the ratio found between the average $\mathrm{AET_{Turc}}$ and the initial $K_c\mathrm{ET_0}$ estimate. The improved AET estimate is $\mathrm{AET} = \alpha_{\mathrm{AET}} \cdot K_{\mathrm{c}}\mathrm{ET_0}$ where α_{AET} is the scaling AET factor provided in Table 4. While this scaling factor is assumed to be constant throughout the year, hourly variation (hourly $\mathrm{ET_0}$ signal) and seasonal variations (seasonal K_{c}) of AET are considered. Assuming one mean annual value of α_{AET} is coarse, as strong seasonal variations in AET signal are expected due to the seasonal variations of $\mathrm{ET_0}$ and vegetation activity, but water balances (and thus α_{AET} estimates) would be more uncertain over shorter periods. Table 4 shows the results of data rescaling for catchments #2, #3 and #4 that have unrealistic mass balances. It gives the values of the computed rescaled $\mathrm{AET_{Turc}}$ and the corresponding computed mean annual precipitation (P_{Turc}). In addition, scaling parameter values α_{AET} and α_P are given for each considered catchment. We consider the rescaled runoff coefficients to be more realistic, as they are closer to those of catchment #1, where the water balance is consistent with Turc (1951) AET.

The new precipitation and new AET values for catchments #2, #3 and #4 are then used in further analysis, whereas original data were conserved only for catchment #1.

3 Methodology

In this part, we first present the estimation of the discharge sensitivity function, $g(Q)$, which is used to characterize the catchment hydrological response. Then we assess whether the estimated $g(Q)$ is really representative of the catchment behaviour using two additional calculations. First, a simple bucket deterministic model is built for the various examined sub-catchments and simulated discharge is compared to observations. Second, rainfall catchment amounts are retrieved from discharge fluctuations ("doing hydrology backwards") and compared to independent observations. Afterwards, we present a sensitivity analysis showing the impact of the parameters of the $g(Q)$ function on the results. Finally, simple dynamical systems approach is used with non-rescaled pre-

cipitation and evapotranspiration data to show how data inconsistency problems may affect discharge simulations.

3.1 Estimation of the sensitivity function $g(Q)$

Kirchner (2009) proposed a method for determining nonlinear reservoir parameters for a simple bucket model with the assumption that discharge Q depends uniquely on total water storage S in the catchment. The analysis starts, as many parametric rainfall–runoff models do, with the water balance equation, in which the total catchment storage variation is estimated using

$$\frac{\mathrm{d}S}{\mathrm{d}t} = P - \mathrm{AET} - Q, \tag{5}$$

where S is water storage volume (L) and P, AET and Q are rates of precipitation, actual evapotranspiration and discharge, respectively ($L\,T^{-1}$). Q, P, AET and S are considered as functions of time and considered to be averaged over the whole catchment (Kirchner, 2009).

It is known that precipitation measurements are spatially variable. Rain gauges reflect precipitation on areas much smaller than the catchment itself. The same comment is valid for evapotranspiration estimates, which are typically representative of much smaller areas than the catchment.

In Eq. (5), only discharge can be considered as a state variable that characterizes the entire catchment. This observation led Kirchner (2009) to make the fundamental assumption that discharge is uniquely dependent on total water storage S in the catchment, and that therefore

$$Q = f(S) \text{ or } S = f^{-1}(Q). \tag{6}$$

Differentiating Eq. (6) with respect to time, one obtains:

$$\frac{\mathrm{d}Q}{\mathrm{d}t} = \frac{\mathrm{d}Q}{\mathrm{d}S}\frac{\mathrm{d}S}{\mathrm{d}t} = \frac{\mathrm{d}Q}{\mathrm{d}S}(P - \mathrm{AET} - Q), \tag{7}$$

and $\mathrm{d}Q/\mathrm{d}S$ can also be expressed as a function of Q, following Kirchner (2009), as

$$\frac{\mathrm{d}Q}{\mathrm{d}S} = f'(S) = f'(f^{-1}(Q)) = g(Q), \tag{8}$$

where $g(Q)$ is the "sensitivity function" as defined in Kirchner (2009). It describes the sensitivity of discharge to changes in storage, as a function of discharge itself. This is useful because discharge is directly measurable whereas whole-catchment storage is not.

Combining Eqs. (7) and (8) we can express $g(Q)$ as Kirchner (2009):

$$g(Q) = \frac{\mathrm{d}Q}{\mathrm{d}S} = \frac{\mathrm{d}Q/\mathrm{d}t}{\mathrm{d}S/\mathrm{d}t} = \frac{\mathrm{d}Q/\mathrm{d}t}{P - \mathrm{AET} - Q}, \tag{9}$$

where the sensitivity function can be described using precipitation (P), actual evapotranspiration (AET), discharge (Q) and rate of change of discharge ($\mathrm{d}Q/\mathrm{d}t$).

Following the approach of Kirchner (2009), we consider periods when precipitation and actual evapotranspiration are relatively small compared to discharge, obtaining the following equation, which shows that under these conditions the discharge sensitivity function can be estimated from discharge data alone:

$$g(Q) = \frac{\mathrm{d}Q}{\mathrm{d}S} \approx -\frac{\mathrm{d}Q/\mathrm{d}t}{Q}\Big|_{P \ll Q, \mathrm{AET} \ll Q}. \tag{10}$$

We select hourly records for nighttime (defined as the period between sunset and sunrise) during which the total rainfall is less than 0.1 mm within the preceding 6 h and following 2 h (Krier et al., 2012). We also tested larger time windows (10 and 12 h instead of 8 h) which did not improve $g(Q)$ estimation.

The sensitivity function $g(Q)$ is estimated using discharge records from low-vegetation periods (from November to March) from 2000 until 2008, when vegetation and ET_0 could be considered to have a smaller impact on stream discharge. Melsen et al. (2014) also pointed out the importance of selecting the low-vegetation periods for estimating the $g(Q)$ function due to the high evapotranspiration conditions in the rest of the year. They also suggest that one winter season could be enough to get a robust estimate of $g(Q)$. Given the larger catchment size and larger climate variability in our catchment, we use the whole low-vegetation period from 2000–2008 for this estimation. Later, the resulting $g(Q)$ function was nevertheless used for precipitation retrieval and discharge simulation during both low-vegetation and vegetation periods (April–October).

We avoid the vegetation period for the estimation of the $g(Q)$ function since, as Fig. 3 shows, during this period ET_0 is much larger than discharge, and the Ardèche catchments clearly respond to ET_0 forcing during the entire 24 h period. In addition, in the Ardèche Basin, the diurnal amplitude (computed as half the difference between the daily maximum and minimum flow) often exceeds 20 % of the daily average flow.

These rainless nighttime hours are further used to determine the sensitivity function $g(Q)$ by constructing "recession plots" (Brutsaert and Nieber, 1977) of the flow recession rate ($-\mathrm{d}Q/\mathrm{d}t$) as a function of discharge. Following Brutsaert and Nieber (1977) and Kirchner (2009), the flow recession rate is estimated as the difference between two successive hours as:

$$-\frac{\mathrm{d}Q}{\mathrm{d}t} = \frac{(Q_{t-\Delta t} - Q_t)}{\Delta t}. \tag{11}$$

Then, the discharge is averaged over those 2 hours as $(Q_{t-\Delta t} + Q_t)/2$. Binning is then done by grouping the individual hourly data into ranges of Q and then calculating the mean and standard error for $-\mathrm{d}Q/\mathrm{d}t$ and Q for each bin. Following Kirchner (2009), values of $-\mathrm{d}Q/\mathrm{d}t \leq 0$ are also included in the binning analysis to avoid the introduction of bias. The bin size was initially set at 1 % of the logarithmic

range in Q but was locally increased if necessary to bring the standard error of $-\mathrm{d}Q/\mathrm{d}t$ down to 50 % of the mean $-\mathrm{d}Q/\mathrm{d}t$ (Kirchner, 2009).

A quadratic function (Kirchner, 2009) is then fitted to the binned means leading to the following empirical equation in log space:

$$\ln(g(Q)) = \ln\left(-\frac{\mathrm{d}Q/\mathrm{d}t}{Q}\Big|_{P \ll Q, \mathrm{AET} \ll Q}\right)$$
$$\approx C_1 + C_2 \ln(Q) + C_3 (\ln(Q))^2. \quad (12)$$

As noted by Kirchner (2009), the C_2 parameter in Eq. (12) is one less than the linear term in a regression fit to the binned $\ln(-\mathrm{d}Q/\mathrm{d}t)$ versus $\ln(Q)$ plot.

3.2 Discharge simulation

Discharge sensitivity functions can be used to simulate discharge (Kirchner, 2009) by combining Eqs. (9) and (10), resulting in the following expression, where the quadratic function of Eq. (12) is used to describe $g(Q)$:

$$\frac{\mathrm{d}Q}{\mathrm{d}t} = \frac{\mathrm{d}Q}{\mathrm{d}S}\frac{\mathrm{d}S}{\mathrm{d}t} = g(Q)(P - \mathrm{AET} - Q). \quad (13)$$

In solving Eq. (13), attention is paid to two details: time lags and numerical instabilities (Kirchner, 2009). A time lag is introduced to account for flow routing delays between changes in catchment storage and changes in discharge at the outlet. Changes in subsurface storage could also lag behind rainfall inputs due to the delays necessary for rainfall to infiltrate and change discharge at the outlet. However, these time lags do not affect the estimation $g(Q)$ since Q and $\mathrm{d}Q/\mathrm{d}t$ are measured simultaneously at the catchment outlet.

Equation (13) indicates that dQ/dt depends on the balance between precipitation, actual evapotranspiration and discharge. However, variations in $P - \mathrm{AET} - Q$ are mainly forced by variations in precipitation. For instance, in the Ardèche at Meyras (#1) catchment, the variance of hourly precipitation is over 15 times larger than the variance of hourly discharge and around 80 times larger than the variance of hourly evapotranspiration. In discharge simulations, lag time is not of such importance since discharge is highly auto-correlated. However, in precipitation retrieval, lag time is taken into account to enhance model performance (see Sect. 3.3 for more details) because precipitation varies more on short timescales.

In order to minimize numerical instabilities, Eq. (13) is solved using its log transform (Kirchner, 2009):

$$\frac{d(\ln(Q))}{\mathrm{d}t} = \frac{1}{Q}\frac{\mathrm{d}Q}{\mathrm{d}t} = \frac{g(Q)}{Q}(P - \mathrm{AET} - Q)$$
$$= g(Q)\left(\frac{P - \mathrm{AET}}{Q} - 1\right). \quad (14)$$

Equation (14) is then computed using fourth-order Runge–Kutta integration, iterating on an hourly time step. A single value of measured discharge is used to initialize the simulation. In addition, Kirchner (2009) also remarked that solution can be unstable unless the parameter C_3 of Eq. (12) is less than 0.

To estimate the AET term in Eq. (14), Kirchner (2009) originally used Penman–Monteith reference evapotranspiration and a rescaling effective parameter (k_e) that was calibrated for the entire study period. Other authors have used slight variants of this approach: Teuling et al. (2010) used the Priestley–Taylor equation to estimate catchment-scale evapotranspiration, defining the evaporation efficiency as a fitting parameter; Brauer et al. (2013) used a parameter f that takes into account the difference between potential and actual evapotranspiration on a monthly basis.

In our study, we assumed that actual evapotranspiration is equal to potential evapotranspiration (PET) throughout the year, being defined as reference evapotranspiration ET_0 modulated by a crop coefficient depending on the nature of vegetation for each catchment (Eq. 1). The strong hypothesis that $\mathrm{AET} = \mathrm{PET}$ is likely to be more relevant in winter, when there is sufficient water content in the air and soils, than in summer. For example, Boronina et al. (2005) found that in Cyprus, actual evapotranspiration was close to potential rate during the November–March period since there was always water present in the air and soils. Nonetheless we use this assumption, even in summer, as a first rough approximation in order to assess the feasibility of such a simple modelling concept. For the application to the Ardèche catchment, as mentioned in Sect. 2.2.1, we assumed that AET was given by Eq. (1), computed on an hourly time step. According to the catchment, either the original $K_C\mathrm{ET}_0$ (catchment #1) or rescaled $\alpha_{\mathrm{AET}}K_C\mathrm{ET}_0$ (catchments #2, #3, #4) were used.

To show how data inconsistency problems may affect the performance of discharge simulation, we also ran the model with non-rescaled values of precipitation and evapotranspiration. The resulting model performance is reported in Sect. 4.5.

3.3 Rainfall retrieval based on $g(Q)$

Until recently, it was considered infeasible to infer precipitation from streamflow fluctuations. Spatial variability of precipitation is high and conventional rain gauges can only measure precipitation over an area that is many orders of magnitude smaller than a catchment itself. We assess the relevance of the inferred storage–discharge relationship for the examined catchments in the Ardèche using the rainfall retrieval scheme ("doing hydrology backward") as proposed by Kirchner (2009) and further tested by Krier et al. (2012).

Assuming that the assumptions of the SDSA are valid, we can infer temporal patterns of precipitation rates from streamflow fluctuations using the following inversion of Eq. (13), as outlined by Kirchner (2009):

$$P - \mathrm{AET} = \frac{\mathrm{d}S}{\mathrm{d}t} + Q = \frac{\mathrm{d}Q/\mathrm{d}t}{\mathrm{d}Q/S} + Q = \frac{\mathrm{d}Q/\mathrm{d}t}{g(Q)} + Q. \quad (15)$$

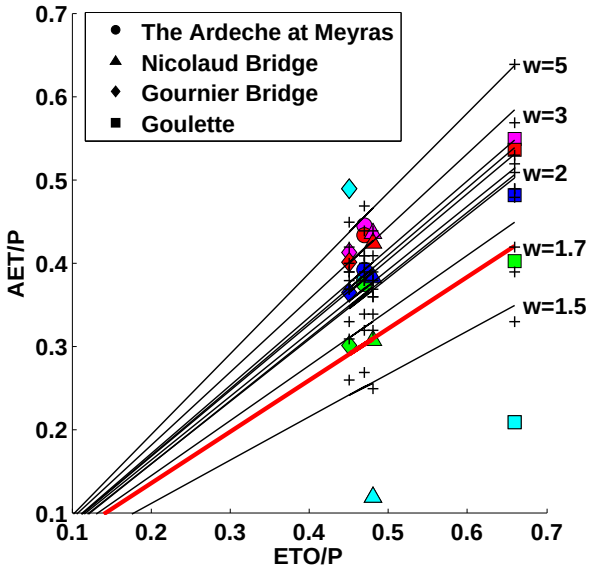

Figure 4. Mean annual evapotranspiration ratio AET / P as a function of the dryness index ET_0 / P for different values of parameter w, using the Fu (1981) curve and different formulas (Turc, Schreiber, Pike, Budyko; see Table 5). Colours correspond to different formulas (cyan = original data; green = Turc, blue = Schreiber, pink = Pike, red = Budyko) and shapes represent different examined catchments.

To apply this concept, one must take account of the travel time lag between changes in discharge from the hillslope and changes in streamflow at the outlet. A time lag l is used for this purpose leading to the following equation (Kirchner, 2009):

$$P - \mathrm{AET} \approx \frac{(Q_{t+l+1} - Q_{t+l-1})/2}{\left[g(Q_{t+l+1}) + g(Q_{t+l-1})\right]/2} + (Q_{t+l+1} - Q_{t+l-1})/2, \quad (16)$$

where l is the travel time lag.

The time lag is optimized for each sub-catchment by calculating the correlation coefficient between estimated and measured rainfall using the lag times of 1, 2, 3, 4, 5, 6, 12, 24 and 48 h. The lag time that shows the best correlation is used. This approach is similar to the one used by Krier et al. (2012).

To make this concept of "doing hydrology backward" feasible, we identify periods when the contribution of evapotranspiration in the water balance equation can be neglected. This includes rainy periods when relative humidity should be relatively high, resulting in low evapotranspiration fluxes and thus P-AET $\approx P$. Based on this assumption, precipitation rates can be directly deduced from the streamflow fluctuations using the following formula (Kirchner, 2009):

$$P \approx \mathrm{MAX}\left(0, \frac{(Q_{t+l+1} - Q_{t+l-1})/2}{\left[g(Q_{t+l+1}) + g(Q_{t+l-1})\right]/2} + (Q_{t+l+1} - Q_{t+l-1})/2\right), \quad (17)$$

where P is the precipitation rate retrieved from discharge fluctuations with time lag l.

To measure the agreement between the reference values and the retrieved values we use the coefficient of determination R^2 (see Sect. 3.4 for more details). The reference precipitation is defined as a combination of local rain gauging and SAFRAN estimates depending on the sub-catchment being examined (see Sect. 2.2).

3.4 Comparison between observed and simulated/retrieved values

To assess model efficiency, we use Nash–Sutcliffe efficiency and percent bias as model evaluation criteria for discharge simulations, and coefficient of determination for rainfall retrieval. Nash–Sutcliffe efficiency, NSE (Nash and Sutcliffe, 1970) is used as a dimensionless model evaluation statistic indicating how well the simulated discharges fit the observations. We compute the NSE to emphasize the high flows as shown in the following equation:

$$\mathrm{NSE} = 1 - \left(\frac{\sum_{i=1}^{n}\left(Y_i^{\mathrm{obs}} - Y_i^{\mathrm{sim}}\right)^2}{\sum_{i=1}^{n}\left(Y_i^{\mathrm{obs}} - Y^{\mathrm{mean}}\right)^2}\right), \quad (18)$$

where Y_i^{obs} is the ith observation of discharge data, Y_i^{sim} is the simulated discharge value for ith time step, Y^{mean} is the mean of all observed data and n represents the number of observations.

NSE values range between $-\infty$ and 1.0, with 1 representing the optimal value (see Moriasi et al., 2007, for a recent review of performance criteria). We also computed NSE on the logarithm of the discharge to give less weight to the peaks.

In addition, percent bias (PBIAS) was also calculated as a part of the model evaluation statistics. It measures total volume difference between two time series, as Eq. (19) indicates:

$$\mathrm{PBIAS} = \frac{\sum_{i=1}^{n}(Y_i^{\mathrm{obs}} - Y_i^{\mathrm{sim}}) \cdot 100}{\sum_{i=1}^{n}(Y_i^{\mathrm{obs}})}, \quad (19)$$

where Y_i^{obs} is the ith observation of discharge data, Y_i^{sim} is the simulated discharge value for the ith time step, n represents the number of observations and 100 converts the result to percent.

The optimal value of PBIAS is 0.0 where positive values indicate model overestimation bias, and negative values indicate model underestimation bias (e.g. Gupta et al., 1999).

In rainfall retrieval, model performance is assessed by using the coefficient of determination (R^2) to quantify the linear correlation between observed and inferred precipitation. R^2 ranges from 0 to 1, where higher values indicate smaller error variance (e.g. Moriasi et al., 2007). Although the inversion formula yields individual hourly values (Eq. 14), we use daily averages to compute R^2. This is done to reduce the effects of small discrepancies in timing that become less consequential when R^2 is calculated on a daily time step (Kirchner, 2009).

3.5 Sensitivity analysis

In this part, we performed a Monte Carlo analysis to sample the parameter space defined by the three parameters C_1, C_2 and C_3 and investigate further whether the values derived from streamflow fluctuations are representative, and how these parameters impact streamflow simulations. This Monte Carlo sensitivity study was conducted for the Ardèche at Meyras (#1) catchment.

A representative set of 10 000 (C_1, C_2, C_3) triplets was sampled randomly from the a priori defined parameter ranges (see Sect. 4.4 for more details) using Monte Carlo methods. Then the discharge was simulated using the model presented in Sect. 3.2 and Eq. (14). We used the NSE (ln for low flow and linear for high flows) to measure the similarity between the simulated and observed discharge. Then we verified that the parameter set derived from data is in the range of the sets leading to the best agreement between model and observations.

The number of simulations (10 000) was assumed to be adequate in view of the relative simplicity of the parametric model, and because the best-fit NSE did not change significantly beyond 10 000 simulations. For comparison, Zhang et al. (2008) and Tekleab et al. (2011) used 20 000 simulations for a four-parameter dynamic water balance model, and Uhlenbrook et al. (1999) used more than 400 000 model runs for the much more complex HBV model with 12 parameters.

4 Results

The results section is divided into five parts. In the first part, results concerning estimation of $g(Q)$ function and its sensitivity analysis are given. Then we present the assessment of the relevance of this estimated $g(Q)$ function by examining the accuracy of the simulated discharge (Sect. 4.2) and retrieved precipitation (Sect. 4.3). In Sect. 4.4, the impact of parameter variations on the simulated hydrographs and results of the Monte Carlo simulations are shown. Finally, the results with non-scaled original data are presented in Sect. 4.5.

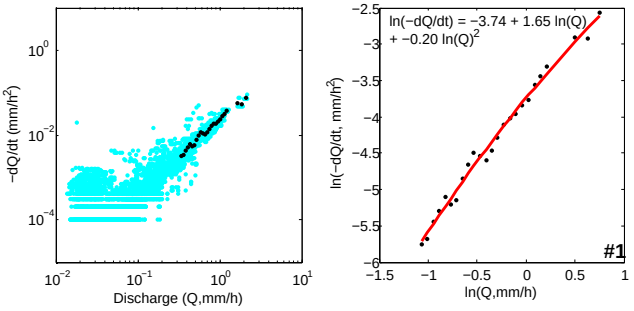

Figure 5. Recession plots for the Ardèche at Meyras (#1) catchment for all low-vegetation periods between 2000 and 2008: left, flow recession rates ($-\mathrm{d}Q\,/\,\mathrm{d}t$) as a function of flow (Q) for individual rainless night hours (blue dots) and their binned averages (black dots); right, quadratic curve fitting with binned means.

4.1 $g(Q)$ estimation

Figure 5 shows an example of a recession plot for the Ardèche at Meyras (#1) catchment for the all low-vegetation periods between 2000 and 2008. We observe that the recession plot exhibits large scatter at low discharge. This result is consistent with the findings of Kirchner (2009) and Teuling et al. (2010). They argue that this is possibly due to measurement errors or differences between the modelling concept and reality.

Table 6 provides values of the recession plot parameters for all four catchments during low-vegetation periods between 2000 and 2008. It shows one parameter set for each catchment. We observe that our choice of the low-vegetation period for estimation of $g(Q)$ gives consistent results amongst different catchments, with similar values of parameters C_1 and C_2. We also observe that the C_3 parameter, which controls the downward/upward curving of the $g(Q)$ function, is always negative, ranging from -0.02 up to -0.2. This is important because Kirchner (2009) obtained realistic simulated discharge only when recession plots are downward-curving on a log–log scale (meaning the C_3 parameter is negative). Eventually, these parameter sets allowed stable discharge simulation as can be seen in Sect. 4.2.

We have also tested $g(Q)$ estimation for all vegetation periods between 2000 and 2008; during these periods, the C_3 parameter tended to be positive. In this case, when the $g(Q)$ function is extrapolated to very low discharges, very high values of $g(Q)$ are obtained, and thus, numerical instabilities appear that lead to model non-functionality. This is also probably due to the distortion of the discharge time series by evapotranspiration as explained in Sect. 3.1. Melsen et al. (2014) concluded that a two-parameter 'bucket' model is reasonably able to capture high flows but not low flows. In our analysis we used the three-parameter model where the third parameter C_3 is essentially related to the low flows (see Sect. 4.4.1) in order to capture the catchment behaviour in that flow regime.

Table 6. Parameter values for the examined catchments for all low-vegetation periods (2000–2008).

Catchment name (ID)	C_1	C_2	C_3
The Ardèche at Meyras (#1)	−3.74	0.65	−0.2
Borne at Nicolaud Bridge (#2)	−4.08	0.74	−0.15
Thines at Gournier Bridge (#3)	−3.71	0.72	−0.13
Altier at Goulette (#4)	−3.80	0.82	−0.02

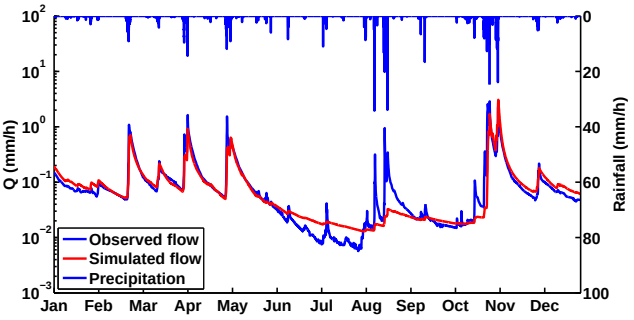

Figure 6. Series of simulated hourly hydrographs (red) for the Ardèche at Meyras (#1) catchment for the year 2004, compared with observed discharge (blue).

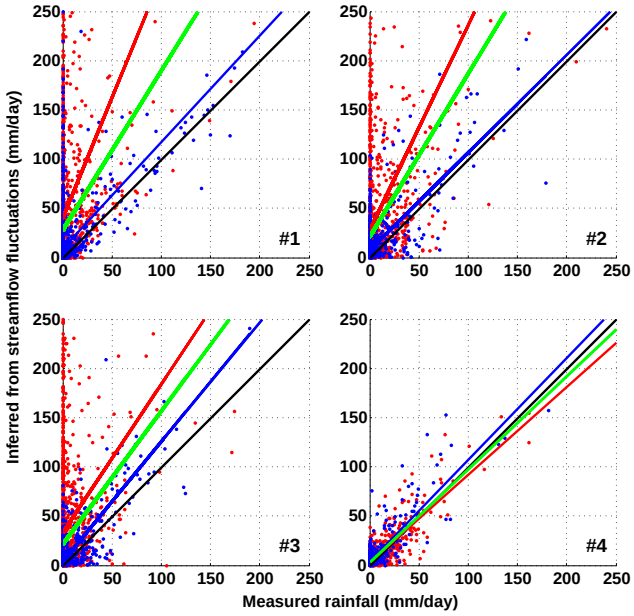

Figure 7. Inferred versus measured daily precipitation for the study catchments: #1. Ardèche at Meyras; #2. Borne at Nicolaud Bridge; #3. Thines at Gournier Bridge; #4. Altier at Goulette. Blue dots correspond to the inferred daily totals from low-vegetation periods; red points correspond to the inferred daily totals from vegetation periods; blue line is correlation for low-vegetation periods, red line for vegetation periods and green line for total examined periods.

4.2 Discharge simulations

Continuous discharge simulations were performed for 2000–2008. Figure 6 presents a simulation extract (year 2004) for the Ardèche at Meyras (#1) catchment. Table 7 presents a model performance summary (NSE, NSE of the logarithm of discharge, and PBIAS) for each catchment and each year.

Looking at Fig. 6, we can see that discharge simulations reproduce the observed hydrograph behaviour better in winter and low-vegetation periods. The low-flow (summer) periods are less well reproduced, even if the overall performance of the simulation is good. The influence of evapotranspiration in summer periods can be one of the explaining factors for that. It should be noted that high evapotranspiration influence is visible only when discharge is evaluated in log space. In linear space, evapotranspiration has a negligible influence on (already quite small) discharge, and the model runs well under dry conditions.

We note in Table 7 that the Ardèche at Meyras (#1) catchment shows satisfactory performance with NSE = 0.68, NSE log = 0.74 and PBIAS of 7.9 % for the 9-year simulation period. Unsatisfactory performance is observed for 2005 (NSE = −0.15, NSE log = 0.07 and PBIAS of 62.2 %). Year 2005 in general can be characterized as a dry year with annual precipitation of 775 mm and annual reference evapotranspiration of 947 mm for this catchment. A mean annual precipitation of 1621 mm and mean evapotranspiration of 809 mm across the examined period (2000–2008) clearly confirms that year 2005 can be considered unusually dry. Table 7 also shows that the year-to-year variations in NSE are very large with some very good results in some years and poor results in other years. This could be a major challenge if the model were to be used for operational purposes.

Furthermore, Gupta et al. (1999) show that PBIAS values for streamflow tend to vary more than other performance criteria between dry and wet years. This could be another possible explanation of the overall poor model performance in 2005 for the Ardèche at Meyras catchment. The Borne at Nicolaud Bridge (#2) and Thines at Gournier Bridge (#3) catchments show good overall performance for the 9-year period with NSE = 0.67 and NSE log = 0.61 and NSE = 0.55 and NSE log = 0.78 respectively. These catchments have stronger variations in PBIAS, however. The last catchment, Altier at Goulette (#4) shows satisfactory model performance with NSE = 0.74 and NSE log = 0.18. It is not known whether the low NSE log value reflects poor model performance or unreliable low-flow discharge data.

4.3 Precipitation retrieval

Following SDSA we retrieved precipitation from discharge fluctuations. We used the same $g(Q)$ derived from the low-vegetation periods (2000–2008) to infer precipitation rates in both vegetation and low-vegetation periods.

The coefficient of determination, mean bias, and slope of the relationship between inferred and measured rainfall for

Table 7. Summary statistics of computed NSE, NSE log and PBIAS for each examined catchment in the Ardèche Basin.

Year	The Ardèche at Meyras (#1)			Borne at Nicolaud Bridge (#2)			Thines at Gournier Bridge (#3)			Altier at Goulette (#4)		
	NSE linear	NSE log	PBIAS (%)	NSE linear	NSE log	PBIAS (%)	NSE linear	NSE log	PBIAS (%)	NSE linear	NSE log	PBIAS (%)
2000	0.60	0.85	−20.7	0.76	0.83	5.02	0.49	0.86	−18.14	0.53	0.70	−1.58
2001	0.61	0.85	5.7	0.59	0.74	33.56	0.27	0.85	−1.43	0.67	0.62	1.86
2002	0.82	0.82	−1.2	0.63	0.53	−12.77	0.68	0.83	−15.05	0.65	0.44	−17.88
2003	0.76	0.72	13.	0.73	0.63	5.78	0.79	0.82	14.27	0.89	−0.19	12.43
2004	0.69	0.86	5.1	−0.07	0.37	−35.28	−0.26	0.78	−18.38	0.42	0.05	−11.09
2005	−0.15	0.07	62.2	0.66	0.64	18.16	0.21	0.53	48.22	0.70	−0.86	0.04
2006	0.51	0.71	19.6	0.68	0.58	0.58	0.36	0.72	17.67	0.18	−0.61	6.90
2007	0.11	0.67	21.8	0.51	0.28	−23.67	0.30	0.71	24.47	−1.22	0.34	−14.48
2008	0.76	0.85	8.2	0.75	0.43	−9.35	0.69	0.79	−6.89	0.83	0.62	6.04
2000–2008	0.68	0.74	7.9	0.67	0.61	0.75	0.55	0.78	0.98	0.74	0.18	−0.29

Table 8. Model performance of inferred versus measured daily rainfall in four sub-catchments for all low-vegetation periods 2000–2008.

Gauging station	R^2	Mean bias ($\mathrm{mm\,day^{-1}}$)	Slope	Time lag (h)
Ardèche at Meyras (#1)	0.41	7.9	1.1	2 (optimized)
Ardèche at Meyras (#1)	0.41	7.9	1.1	1
Borne at Nicolaud Bridge (#2)	0.56	7.4	1.01	2 (optimized)
Thines at Gournier Bridge (#3)	0.61	4.7	1.22	2 (optimized)
Altier at Goulette (#4)	0.71	2	1.09	2
Altier at Goulette (#4)	0.72	2	1.09	1 (optimized)

examined catchments and low-vegetation periods, as well as information about lag time, can be found in Table 8. Other lag times (>2 h) showed poor model performance and are not discussed further in the paper.

Figure 7 shows daily precipitation retrieval for the four studied sub-catchments of the Ardèche during low-vegetation periods, vegetation periods and for the entire study period 2000–2008 using the same $g(Q)$ function estimated from low-vegetation periods (Table 6).

Good correlation between retrieved precipitation and observed precipitation can be observed for low-vegetation periods where the slope of the regression line shows a modest degree of overestimation. Figure 7 illustrates that the inferred precipitation daily totals from low-vegetation periods (blue line) agree quite well with the precipitation measurements in the Altier at Goulette (#4) catchment, yielding R^2 of 0.72. In the other catchments, the inferred precipitation daily totals are well correlated with the either local precipitation measurements or SAFRAN data, showing however sometimes a strong tendency toward overestimation (e.g. the Ardèche at Meyras, #1). Figure 7 also shows strong precipitation overestimation for three examined catchments #1, #2 and #3 in summer periods (red line) and consequently for total examined period, too (green line).

The optimized time lags are generally very small (less than 2 h), which confirms the very short response time in the Ardèche catchment. In order to see whether the retrieved daily rainfalls were sensitive to the lag time, we compared the results obtained with different lag times for two catchments: the Ardèche at Meyras (#1) and Altier at Goulette (#4). The Ardèche at Meyras (#1, 98 $\mathrm{km^2}$) has an optimized lag time of 2 h. We tested the retrieval behaviour with lag times of 1 and 2 h and we observe almost no change in the performance (Table 8): we obtain the same coefficient of determination of 0.41 and a bias of 7.9 $\mathrm{mm\,day^{-1}}$ at a lag time of 1 and 2 h. Similar results are obtained for the Altier at Goulette (#4) catchment, where we observed a slightly better precipitation modelling performance with lag time of 1 h ($R^2 = 0.72$) rather than with a lag time of 2 h ($R^2 = 0.71$).

4.4 Sensitivity analysis

4.4.1 Impact of parameter variations on the simulated hydrographs

As a first approach, a manual sensitivity analysis was done by successively varying the values of each parameter and plotting the corresponding simulated hydrographs (grey areas in Figs. 8 and 9). The results for the Ardèche at Meyras (#1) catchment (year 2004) are presented; see Figs. 8 and 9 for the C_3 and C_1 parameters, respectively. The results for the parameter C_2 are not presented here since this parameter only varies slightly when estimated from low-vegetation periods in each year (see Sect. 4.1) and the results are graphically quite similar to those for the parameter C_1 (but peaks are less affected). The NSE values of log discharge are also calculated (Table 9).

We can see that C_3 seems to be influential during the low-flow summer period and also during recessions of events following low-flow periods (Fig. 8). However, it does not play

Table 9. NSE values of log discharge for the Ardèche at Meyras (#1) catchment, illustrating sensitivity to changes in the C_1 and C_3 parameters. In bold: values obtained from data.

C_1 parameter	NSE on log of discharge	C_3 parameter	NSE on log of discharge
−4	0.81	−0.3	0.68
−3.8	0.85	−0.25	0.79
−3.74	0.86	−0.21	0.85
−3.7	0.86	**−0.2**	0.86
−3.6	0.86	−0.19	0.86
−3.5	0.86	−0.17	0.86
−3.4	0.85	−0.16	0.85
−3.3	0.83	−0.15	0.83
−3.2	0.81	−0.1	0.45
−3	0.71	−0.09	0.26

a significant role in the peaks and in well-established high-flow conditions. In contrast, the C_1 parameter has an important influence on the whole hydrograph (Fig. 9), including the peaks. Low values of C_3 tend to flatten the model response, causing overestimated low-flow values and underestimated peaks.

From Table 9 we can also observe that the model efficiency for the parameter values that were obtained from the recession plots is close to optimal (at least for this year at this site), and cannot be substantially improved by manual parameter adjustments.

4.4.2 Exploration of parameter range using Monte Carlo simulations

In order to complement the manual sensitivity analysis presented above, to explore the range of these parameters and to assess whether the parameters of the $g(Q)$ function derived from data analysis are representative, we performed Monte Carlo simulations using the model described by Eq. (14) with randomly sampled values of the three parameters C_1, C_2 and C_3. The parameters were sampled randomly from the a priori defined parameter range given in Table 10. For each simulation, the NSE and NSE log (on the log of discharge) were calculated to assess the performance of the parameter set. The results are presented using dotty plots for the Ardèche at Meyras (#1) catchment in Fig. 10. Table 10 also indicates the range of "behavioural" values for each parameter as derived from the dotty plots, defined as the range where NSE is higher than 0.7, along with the values derived from the recession plots.

The results show that when the parameters are calibrated to discharge simulations, their ranges are quite large. The maximum model performance appears to be around 0.8 for all three parameters and both indicators. Low-flow performance (NSE log) is not very sensitive to the variations of the parameters. Giving peak flow more weight (NSE) allows the identification of clear optima and a narrower range for the C_1 parameter. Concerning the C_2 parameter, although the initial guess of the parameter range was quite narrow (see Table 10), the final "optimized" range is almost the same, with no clear optimum. For the C_3 parameter, the final "optimized" range is found to be half of the initial one. These two parameters appear thus to be not very sensitive, although the sign of the C_3 parameter was already identified as a key element of successful discharge simulations. Finally, the parameter values obtained from recession plots are in the optimized parameter range, thus suggesting that the analysis of discharge recessions is sufficiently informative and that there is no need of additional model calibration for discharge simulation. Beven and Binley (1992) have argued that having too many parameters increases the degrees of freedom beyond what data can properly deal with; this results in having different sets of parameters that give similar results (the equifinality problem). Figure 10 shows that although conventional parameter calibration leads to substantial equifinality (particularly for the C_2 parameter), the parameter values obtained from the recession plots fit well within the "behavioural" parameter range from the Monte Carlo analysis. Our analysis shows that the recession plots yield parameter estimates that are consistent with (and arguably better constrained than) parameter values obtained from conventional model calibration methods.

4.5 Modelling performance with non-scaled original data

In Sect. 2.3 we introduced a rescaling technique to obtain more representative water balances for catchments #2, #3 and #4. Here, we show the consequences of foregoing this rescaling for those three catchments that showed unrealistic mass balances (Table 3). Figure 11 shows observed discharge and simulated hourly hydrographs for the Altier at Goulette (#4) catchment for the year 2000, obtained with non-scaled data, rescaling of precipitation alone, and rescaling of both precipitation and evapotranspiration.

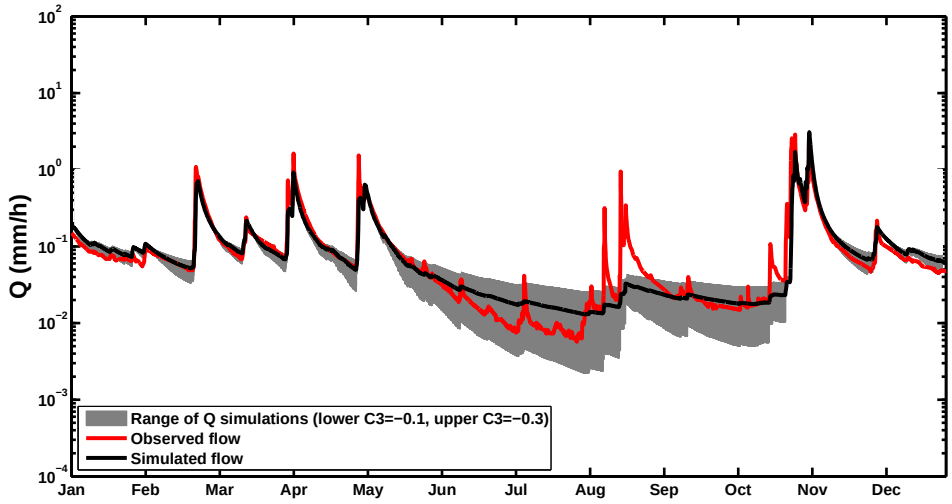

Figure 8. Observed versus simulated hydrograph ($C_3 = -0.2$) for the Ardèche at Meyras (#1) catchment (year 2004), with C_3 parameter variations (C_1 and C_2 values are kept constant at (-3.74) and 0.65, respectively). The grey area shows the range of discharge simulations.

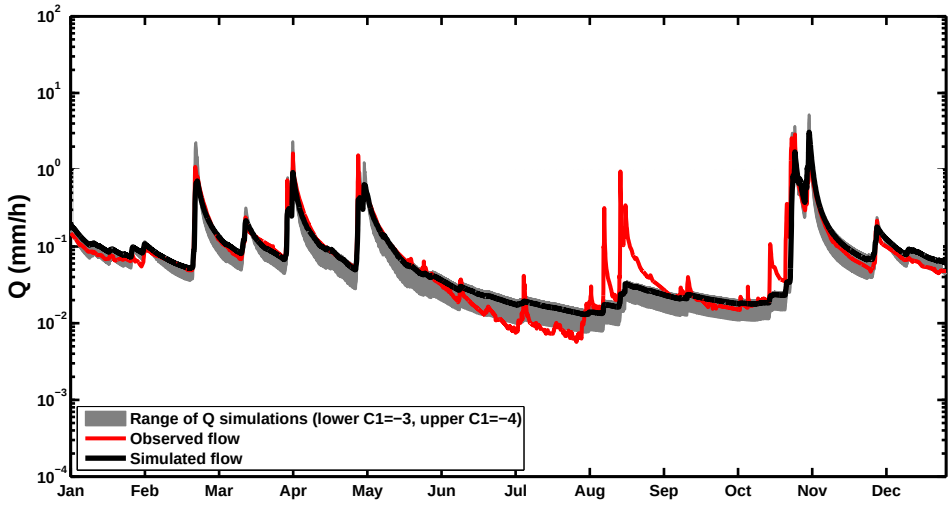

Figure 9. Observed versus simulated hydrograph ($C_1 = -3.74$) for the Ardèche at Meyras (#1) catchment (year 2004) with C_1 parameter variations (C_2 and C_3 values are kept constant at 0.65 and -0.2, respectively). The grey area shows the range of discharge simulations.

The lack of water balance closure may contribute substantially to poor model performance, as can be seen from Fig. 11. The simple dynamical systems approach, like many modelling approaches, is based on conservation of mass; it is therefore unsurprising that it may perform poorly when tested against data sets that violate mass conservation. We observe that when the original non-scaled data are used, discharge is generally underestimated. By introducing the rescaled precipitation, flow peaks can be better reproduced, but model performance is still poor during the vegetation period. If both the rescaled evapotranspiration and rescaled precipitation are used, significantly better results are obtained in both vegetation and low-vegetation periods.

As a complement to assessing modelling performance with non-scaled data, we re-ran the SDSA model for these catchments to see how this affects the hydrograph simulation and performance indicators. Table 11 compares model performance with the original operational data and the rescaled data, using NSE, NSE on log of discharge and PBIAS as performance metrics. We observe that model performance is markedly improved by using the rescaled precipitation as forcing (runoff coefficients are more representative as shown in Table 4). In addition, model performance is improved by also introducing rescaled evapotranspiration (better NSE and lower PBIAS values are obtained).

Table 10. Comparison of the chosen parameter range and parameters obtained from low-vegetation periods for the Ardèche at Meyras (#1) catchment.

Parameters	C_1	C_2	C_3
Parameter range	[−1]–[−6]	[0.1–1]	[−0.001]–[−0.5]
The range of "behavioural" values	[−3.5]–[−4.5]	[0.1–0.9]	[−0.001]–[−0.25]
Reference (from recession plots)	−3.74	0.65	−0.2

Table 11. Model performance for three examined catchments over the whole examined period (2000–2008), comparing the original operational data and rescaled precipitation and evapotranspiration data.

Catchment	Performance	Operational	Rescaled P	Rescaled P and AET
Borne at Nicolaud Bridge (#2)	NSE	0.45	0.65	0.67
	NSE log	0.58	0.70	0.61
	PBIAS	42	14.2	0.75
Thines at Gournier Bridge (#3)	NSE	0.36	0.50	0.55
	NSE log	0.79	0.62	0.78
	PBIAS	−13.8	22	0.98
Altier at Goulette (#4)	NSE	0.54	0.79	0.74
	NSE log	−4.90	−2.99	0.18
	PBIAS	49	23.65	−0.29

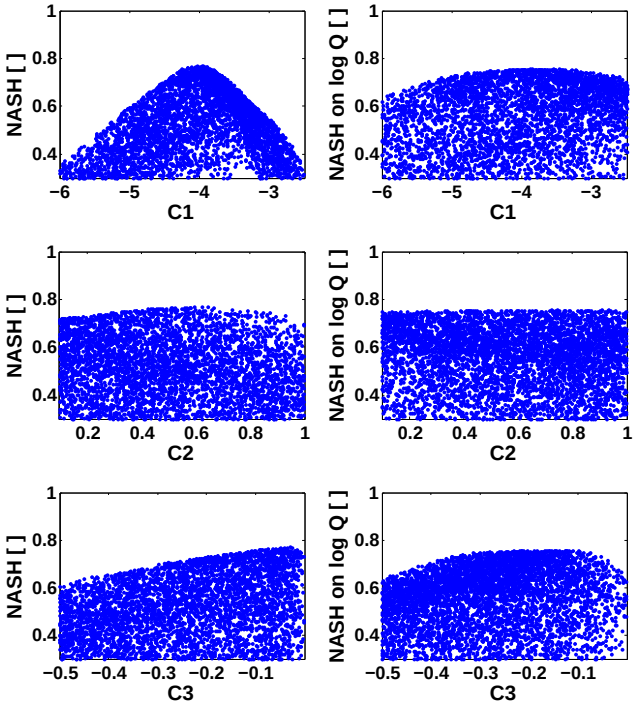

Figure 10. Dotty plots for the Ardèche at Meyras (#1) catchment (left: plots with NSE efficiencies; right: plots with NSE efficiencies calculated on log Q).

5 Discussion

In this study, the SDSA method was applied to four subcatchments in the Ardèche catchment (France), representative of Western Mediterranean catchments. We first discuss the advantages and limits of the method for this type of catchment. Then we discuss how the application of this approach was useful in deriving information about the catchment functioning and possible dominant processes.

5.1 About the applicability of the SDSA to Mediterranean type catchments

The application of this method to the Ardèche catchment was at first quite challenging. In particular, the basins are larger and less humid than those of the original case studies; in addition, data availability is more limited and data quality is distinctly lower.

5.1.1 Drainage area

The drainage area does not seem to be a limiting factor at the scale of our catchments. The catchments where this theory has been applied so far in order to reproduce the hydrograph were typically smaller than ∼10 km^2. In our study, the sizes of the studied catchments varied from 16 km^2 to 103 km^2 and SDSA performance was not correlated to the size of the catchment. Krier et al. (2012) report that when this approach is used for "doing hydrology backward" to retrieve rainfall amounts, the model performance in larger basins is as good as or sometimes even better than in smaller catch-

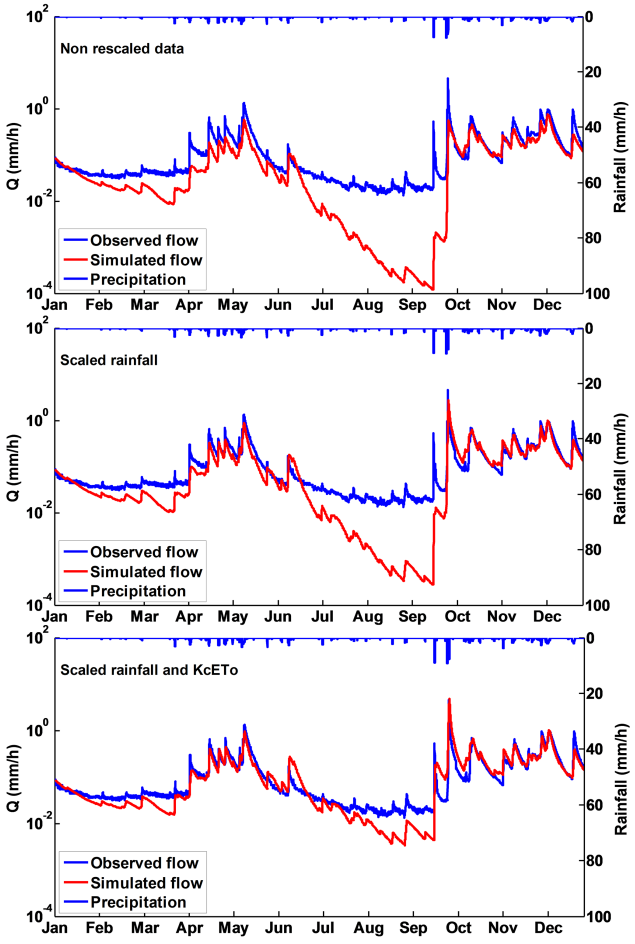

Figure 11. Series of simulated hourly hydrographs (red) for Altier at Goulette (#4) catchment for the year 2000 and its comparison with observed discharge (blue), using original non-scaled data (top), with rescaled P only (middle), and rescaled P and K_c ET_0 (bottom).

ments. Kirchner (2009) also addressed this issue arguing that the approach was unlikely to work for catchments that are too big (e.g. more than 1000 km^2). This is due to the lag times required for changes in discharge to reach the outlet; in such large catchments these lag times would be so long and variable that the model would be likely to fail. In addition, the theory presented here could not be expected to work in the catchments that are bigger than the scale of individual storms (Kirchner, 2009). Suggestions for how to deal with large river basins are given in Sect. 6.

5.1.2 Data quality

Our study demonstrates that data quality is particularly important for the application of this method. Concerning discharge data, the method is based on the discharge-sensitivity function $g(Q)$, and discharge measurement errors consequently will lead to biases in the appraisal of the catchment functioning. In catchments with artificial reservoirs/dams the assumption of a unique storage–discharge relation will not hold from the SDSA point of view. Thus this will limit the applicability of the SDSA method (and many other catchment models) in practice.

In the present study, we used discharge data from operational networks. We have shown in Sect. 2.2 that there are known issues with the quality of these data for our purposes. Nevertheless, when data consistency is sufficient (e.g. Ardèche at Meyras (#1) station), a robust estimation of the $g(Q)$ function from low-vegetation periods can be obtained, leading to accurate simulation of the discharge. In addition, we would like to emphasize that the discharge sensitivity function $g(Q)$ only depends on discharge. Its estimation is therefore not dependent on the rescaling performed on rainfall and ET_0 data. There is only a minor impact of this rescaling on the selection of points retained for the recession plots; rainfall thresholds are used in this selection, but the results are only marginally impacted by rescaling. On the other hand, rescaling is of paramount importance in the evaluation of the relevance of the estimated $g(Q)$ function using discharge simulation, as shown in Sect. 4.5., because accurate discharge simulations require that mass is conserved.

The quality of the rainfall data was questioned early in our work, and rescaling of precipitation was needed to obtain realistic results. As mentioned in Sect. 2.2, the gridded SAFRAN product underestimates precipitation especially in mountainous areas and underestimates the occurrence of strong precipitation ($P > 20$ mm day^{-1} (Quintana-Seguí et al., 2008; Vidal et al., 2010). As the SAFRAN reanalysis is performed on so-called "symposium zones", assumed to be homogeneous in terms of climate characteristics, overestimation of rainfall is also possible if those zones are inaccurately delineated, as is probably the case for the Thines at Gournier bridge (#3) catchment. Some authors tried to overcome the rainfall underestimation problem in mountainous areas by interpolating the SAFRAN data across altitude bands (Etchevers et al., 2001; Lafaysse et al., 2011; Thierion et al., 2012), but these data were not available for the present study. In addition, SAFRAN re-analyses are based on existing rain gauges. In mountainous areas, the few rain gauges that do exist are generally located in lower, flatter terrain, and may not capture the increase of rainfall with altitude that has been identified in this region (Molinié et al., 2011). It would be interesting to assess the performance of the "hydrology backwards" rainfall inversion using more accurate rainfall estimates as reference. As reference daily rainfall, we propose to use the SPAZM reanalysis (Gottardi, 2009), which improves rainfall estimation in mountainous area, when it becomes available to us.

Assuming that the discharge data are reliable, it was shown that when input rainfall and ET_0 consistent with the water balance closure are used, the discharge simulated using the $g(Q)$ function is much more accurate than with the original input data. Coussot (2015) generalized the study presented in

this paper to about 20 catchments of the Cévennes region and found the same kind of water balance closure problems as in our study. Once rescaling of rainfall and ET_0 was performed, he obtained similar results as those presented in this paper.

One assumption behind the rescaling approach proposed in Sect. 2.2.2 is that discharge data are reliable enough to provide an accurate estimate of annual runoff. This is of course questionable, because stage–discharge relationships are known to be highly extrapolated in this region due to the difficulty of gauging high discharges (e.g. Le Coz et al., 2010). As also mentioned in Sect. 2.2.1, low discharges are also highly uncertain, because these stations were often designed for flood warning purposes. Work is currently in progress in order to quantify the runoff data accuracy. This work is based on the BaRatin method (Le Coz et al., 2014) which provides an uncertainty range on the estimated discharge. The uncertainty can be propagated to the whole discharge time series (Branger et al., 2015) and the next step will be the propagation to the hydrological water balance and the quantification of uncertainty for the annual and monthly values. This work will help quantify which of the data (rainfall, discharge or both) need to be improved.

In addition, the operational discharge measurement network has recently been complemented by research instrumentation covering nested scales (see Braud et al., 2014 for details). In particular, small catchments ranging from 0.5 to 100 km^2 have been monitored continuously since 2010. The data set was not long enough to be used in the present study, but these new data are expected to be of higher accuracy than the operational data used in this study, so that they can provide additional insight into the hydrological response of the catchments.

Regarding discharge uncertainty, if data have to be rescaled, an approach like the one proposed by Yan et al. (2012) should be preferred, as it allows a consolidation of the water balance at the scale of the whole Ardèche catchment, taking into account data uncertainties on all the components, and constraining the results with the water balance equation along the river network.

The simulation results show that additional effort must be put into quantifying data uncertainty in both discharge and rainfall. The derivation of more accurate rainfall fields combining various data sources (such as radar data and in situ gauges (see, for instance, Delrieu et al., 2014) should also be encouraged. It could also be interesting to use actual evapotranspiration estimates derived from remote sensing techniques adapted to complex topography (e.g. Gao et al., 2011; Seiler and Moene, 2010) to obtain independent estimates of AET and better constrain this component in hydrological modelling.

5.1.3 Adequacy of SDSA in our catchment

The sampling strategy of deriving the $g(Q)$ functions from low-vegetation periods appeared to be adequate in our case. We estimated $g(Q)$ by using the streamflow data from low-vegetation periods of the 9-year time series (2000–2008) and then used the resulting parametrization to reproduce the hydrographs (continuous simulations) for the rest of the 9-year interval. This procedure can be understood as a "differential split-sample test" (Klemes, 1986) where the 9-year-long period encompasses different seasonal precipitation variations including wet and dry periods. The results show that the information retrieved from only a fraction of the discharge time series is relevant also for periods with very different characteristics.

Independently from the data quality issues, we also showed that the SDSA model performs better during the wet, winter periods than the dry, summer periods and dry years (see Sect. 4.2). We interpret these results as an indication that the current model is not fully adapted to the high evapotranspiration conditions of our Mediterranean catchments. We must also point out that, when assessing the relevance of the estimated $g(Q)$ function using continuous discharge simulations (Sect. 3.2), it is necessary to provide an estimate of AET. In this first approach, we used the hypothesis that $AET = PET$ where PET is the rescaled $K_C \cdot ET_0$. This assumption is crude because an average annual rescaling factor is used, whereas a monthly value would certainly be more relevant. The method of Thornthwaite and Mather (1955) cited by Gudulas et al. (2013) which provides monthly estimates of AET could be a way to improve our simulations in future works, and an example of application to the Ardèche at Meyras (#1) catchment is provided in Adamovic et al. (2015). Nevertheless, we show in Sect. 4.3 that rainfall retrieval during the vegetation period is poor, confirming the lower performance of the SDSA in this period. The method is therefore less reliable when discharge is low, especially in summer. This is one limitation of the SDSA for dry catchments.

In addition, the recent study of Brauer et al. (2013) showed that the two-parameter model they used cannot deal with complexity of hydrological processes in their catchment (only 39 % of the hydrographs had NSE over 0.5). In the Ardèche catchments, the three-parameter model succeeds in capturing the catchment behaviour, with quite good response of discharge to rainfall in low-vegetation periods (peaks and recession were nicely reproduced).

5.1.4 Interest of the SDSA as compared to other hydrological modelling approaches

Recession analysis has been used to build hydrological models for many years (e.g. Brutsaert and Nieber, 1977). What is new in the SDSA is not the reservoir itself, but the manner to derive its structure and parameters from the data analysis: in particular, here the functional form of the storage–discharge relationship is not specified a priori, but determined directly from data without calibration (Kirchner, 2009). This is the very definition of the top-down or data-driven modelling ap-

proach, that is acknowledged to be a major paradigm shift in modelling by the hydrological community (and which was a major emphasis of the PUB decade; see, for instance, Sivapalan, 2003b and Hrachowitz et al., 2013). We argue that testing this kind of approach on new data sets, for various climatic conditions, contributes to the advance of hydrological science in itself. We have also compared the model results with other models that are based on similar data-driven methodology (e.g. Brauer et al., 2013 and Melsen et al., 2014) and obtained similar results.

The major limitation of the SDSA is of course the availability of good quality discharge data with a short time step, in catchments representative of the spatial variability of hydro-climatic conditions. Discharge must also be representative of natural conditions, which could also limit its applicability in catchments impacted by human activity.

5.2 Catchment functioning hypotheses derived from the analysis

The most important output from our application of the simple dynamical systems approach is the validation of underlying hypotheses and information about the dominant processes that can be derived from the model parametrization.

5.2.1 General considerations

The SDSA model is based on an underlying hypothesis that regards a catchment as a single nonlinear bucket model. In our study we note the good performance of the model in each sub-catchment which suggests that SDSA, although it was developed for humid regions, remains valid for these Mediterranean sub-catchments as well. We can thus interpret that these sub-catchments do follow the model's functioning hypotheses, especially in winter and low-vegetation periods. These results are consistent with the findings of Brauer et al. (2013) for the Hupsel Brook catchment, Kirchner (2009) for Plynlimon and Teuling et al. (2010) for the Rietholzbach catchment. In contrast, during the vegetation period the model seems to be less adapted to our Mediterranean setting. The catchments seem to behave differently when they are dry. This is probably due to the strong influence of evapotranspiration. In our hydroclimatic context (see details in next section), and taking into account that no regional groundwater exists in the Ardèche catchment, discharge provided by the SDSA can be associated with subsurface flow (generally assumed to occur via lateral flow along perched water tables in shallow soils), which is less active in summer and when evapotranspiration is high. It could be necessary to consider another storage, probably more superficial than the "SDSA" storage, which could be used to supply evapotranspiration over shorter timescales, and which may be largely decoupled from subsurface lateral flow that sustains base flows.

5.2.2 Links with physiographic characteristics of the catchments

The model works better in the Ardèche at Meyras (#1) and Thines at Gournier Bridge (#3) catchments, which both are granitic (see Fig. 2). The hypothesis of shallow subsurface flow caused by saturation of at interface between soil and bedrock makes particular sense in this geology (e.g. Cosandey and Didon-Lescot, 1989; Tramblay et al., 2010).

In the forested granitic catchments of this region, infiltration capacity is generally very high and runoff occurs due to soil saturation (e.g. Tramblay et al., 2010). However, this saturation mostly occurs at the interface between the very thin soil and the large altered bedrock, where contrasts of hydraulic conductivity can be encountered, leading to quick lateral subsurface flow. Experiments are currently being conducted on infiltration plots to quantify the velocity of this lateral flow (see Braud et al., 2014 for their description). Therefore the main mechanism we are speaking about is quick lateral subsurface flow which transits through the reservoir considered in the Simple Dynamical Systems Approach. On agricultural areas, in the intermediate part of the Ardèche catchment, infiltration excess surface runoff is likely to occur (and has been observed in the field). Its contribution is also under investigation using detailed experiments (see Braud et al., 2014).

In addition, unaltered bedrock tends to be impermeable, but flow pathways are created in the many fractures, joints and fissures of the altered horizons. During extended rainfall those flow pathways might become connected, generating rapid subsurface flow (Krier et al., 2012). Moreover, the parameter values of the granite catchments are quite similar (see Table 6).

To quantify the relative influence of several predictors of the catchment response (and values of C_1, C_2, C_3 parameters), Adamovic (2014) used factor analysis of mixed data (FAMD). By using this statistical technique along with HCPC (hierarchical clustering on principal components) analysis, geology was found to be the only dominant predictor of runoff variability. The role of geology is more thoroughly demonstrated in Adamovic (2014) for the catchments studied in this paper and in Coussot (2015) for a larger set of catchments from the Cévennes region, but a review of this work is beyond the scope of the present paper.

This is also consistent with the contemporary literature, as geology has been invoked in numerous recent studies as a controlling factor of flood response (Gaál et al., 2012; Garambois et al., 2013; Krier et al., 2012; Vannier et al., 2014). As also discussed by Kirchner (2009), the theory is challenged by catchments with heterogeneous geology and thus with many disconnected subsurface storage reservoirs. This might explain the good modelling performance in granite catchments (see also Vannier (2013) for similar conclusions using a reductionist modelling approach).

6 Conclusion and perspectives

Our study describes in detail the application of SDSA methodology to four catchments of the Ardèche Basin ranging from 16 to 103 km^2, typical of the Western Mediterranean environment.

To have more representative water balance fluxes, we rescaled precipitation and evapotranspiration for three subcatchments (#2, #3 and #4). In our work we used average annual scaling coefficients for the whole time series (for both precipitation and evapotranspiration). In the future, varying the scaling coefficients according to different seasons could possibly lead to a better approximation of hourly precipitation and evapotranspiration fluxes.

We calculated the discharge sensitivity functions from low-vegetation periods and performed continuous discharge simulations with an hourly time step for the period 2000–2008. We also inferred precipitation and performed sensitivity analyses of the three parameters of the discharge sensitivity function.

Our results show that good results for discharge simulation can be obtained, especially under winter humid conditions and for catchments characterized by predominantly granitic lithology. Under dry conditions, poor model performance is mainly related to the disturbed water balance terms, high influence of AET and imprecise discharge measurements. Improving AET estimation is recommended for better model performance in summer periods when evapotranspiration is high and when the unsaturated zone has a significant role in attenuating the precipitation input. Working on the quantification of data accuracy and error reduction is also recommended in order to get more robust and reliable results.

As a perspective to this study, dominant predictors of runoff variability other than geology (such as land use, soil properties, drainage density, topographic steepness etc.) still need to be explored and linked to catchment hydrological behaviour. Relating the obtained parameters of the discharge sensitivity function to the catchment characteristics using different statistical classification techniques (e.g. principal component analysis (PCA) and factor analysis of mixed data (FAMD) or self-organized maps) could allow us to apply the method also to ungauged basins, thus contributing to the PUB initiative (Hrachowitz et al., 2013). Another step would be then to create a distributed "Kirchner type" hydrological model where a parameter set would be attributed to "regions" discretized on the basis of their physiographic characteristics. This would allow us to determine the rainfall–runoff behaviour in large scale river basins by taking into account the precipitation spatial distribution and flood flow routing through the channel network. We would then be able to broaden our understanding of nonlinear catchment response and travel time lags as suggested by Kirchner (2009).

Acknowledgements. The study is conducted within the FloodScale project, funded by the French National Research Agency (ANR) under contract no. ANR 2011 BS56 027, which contributes to the HyMeX program. The HyMeX database teams (ESPRI/IPSL and SEDOO/Observatoire Midi-Pyrénées) helped in accessing the data. The authors acknowledge Brice Boudevillain for providing the OHM-CV rainfall data, Météo-France for their rainfall and SAFRAN climate data. EdF-DTG provided discharge data from three of the gauges used in this study. We thank the Region Rhône-Alpes for its funding of the PhD grant of the first author. We thank R. Krier for providing us the codes used to perform the recession analysis and E. Leblois for constructive comments on the paper.

Edited by: M. Mikos

References

Adamovic, M.: Development of a data-driven distributed hydrological model for regional catchments prone to Mediterranean flash floods. Application to the Ardèche catchment (France), PhD thesis, University of Grenoble, France, 2014.

Adamovic, M. et al.: Interactive comment on "Does the simple dynamical systems approach provide useful information about catchment hydrological functioning in a Mediterranean context? Application to the Ardèche catchment (France)" by M. Adamovic et al., Hydrol. Earth Syst. Sci. Discuss., 11, C6170–C6171, 2015.

Allen, R., Pereira, L., Raes, D., and Smith, M.: Crop evapotranspiration - Guidelines for computing crop water requirements – FAO Irrigation and drainage paper 56, citeulike-article-id:10458368, 1998.

Beven, K. and Binley, A.: The future of distributed models: Model calibration and uncertainty prediction, Hydrol. Proc., 6, 279–298, doi:10.1002/hyp.3360060305, 1992.

Beven, K.: Towards a coherent philosophy for modelling the environment, Proc. Roy. Soc. Lnd. A, 458, 2465–2484, doi:10.1098/rspa.2002.0986, 2002.

Bloschl, G. and Sivapalan, M.: Scale issues in hydrological modelling: a review, Hydrol. Proc., 9, 251–290, 1995.

Bonnifait, L., Delrieu, G., Lay, M. L., Boudevillain, B., Masson, A., Belleudy, P., Gaume, E., and Saulnier, G.-M.: Distributed hydrologic and hydraulic modelling with radar rainfall input: Reconstruction of the 8–9 September 2002 catastrophic flood event in the Gard region, France, Adv. Water Res., 32, 1077–1089, doi:10.1016/j.advwatres.2009.03.007, 2009.

Boronina, A., Golubev, S., and Balderer, W.: Estimation of actual evapotranspiration from an alluvial aquifer of the Kouris catchment (Cyprus) using continuous streamflow records, Hydrol. Proc., 19, 4055–4068, 2005.

Boudevillain, B., Delrieu, G., Galabertier, B., Bonnifait, L., Bouilloud, L., Kirstetter, P.-E., and Mosini, M.-L.: The Cévennes-Vivarais Mediterranean Hydrometeorological Observatory database, Water Resour. Res., 47, W07701, doi:10.1029/2010wr010353, 2011.

Branger, F., Dramais, G., Horner, I., Le Boursicaud, R., Le Coz, J., and Renard, B.: Improving the quantification of flash flood hydrographs and reducing their uncertainty using noncontact

streamgauging methods, EGU General Assembly 2015, Vienna, 12–17 April 2015, Geophys. Res. Abstr., Vol. 17, EGU2015-5768, 2015.

Braud, I., Roux, H., Anquetin, S., Maubourguet, M.-M., Manus, C., Viallet, P., and Dartus, D.: The use of distributed hydrological models for the Gard 2002 flash flood event: Analysis of associated hydrological processes, J. Hydrol., 394, 162–181, doi:10.1016/j.jhydrol.2010.03.033, 2010.

Braud, I., Ayral, P. A., Bouvier, C., Branger, F., Delrieu, G., Le Coz, J., Nord, G., Vandervaere, J. P., Anquetin, S., Adamovic, M., Andrieu, J., Batiot, C., Boudevillain, B., Brunet, P., Carreau, J., Confoland, A., Didon-Lescot, J. F., Domergue, J. M., Douvinet, J., Dramais, G., Freydier, R., Gérard, S., Huza, J., Leblois, E., Le Bourgeois, O., Le Boursicaud, R., Marchand, P., Martin, P., Nottale, L., Patris, N., Renard, B., Seidel, J. L., Taupin, J. D., Vannier, O., Vincendon, B., and Wijbrans, A.: Multi-scale hydrometeorological observation and modelling for flash-flood understanding, Hydrol. Earth Syst. Sci., 11, 1871–1945, doi:10.5194/hessd-11-1871-2014, 2014.

Brauer, C. C., Teuling, A. J., Torfs, P. J. J. F., and Uijlenhoet, R.: Investigating storage-discharge relations in a lowland catchment using hydrograph fitting, recession analysis, and soil moisture data, Water Resour. Res., 49, 4257–4264, doi:10.1002/wrcr.20320, 2013.

Brutsaert, W. and Nieber, J. L.: Regionalized drought flow hydrographs from a mature glaciated plateau, Water Resour. Res., 13, 637–643, doi:10.1029/WR013i003p00637, 1977.

Budyko, M. I.: Climate and life, English Edition, edited by: Miller, D. H., Academic Press, New York, 508 pp., 1974.

Cosandey, C. and Didon-Lescot, J. F.: Etude des crues cevenoles: conditions d'apparition dans un petit bassin forestier sur le versant sud du Mont Lozere, France, International Association of Hydrological Sciences, Wallingford, ROYAUME-UNI, 13 pp., 1989.

Coussot, C.: Assessing and modelling hydrological behaviours of Mediterranean catchments using discharge recession analysis. Master Thesis, HydroHazards, University of Grenoble, France, 54 pp., 2015.

Delrieu, G., Wijbrans, A., Boudevillain, B., Faure, D., Bonnifait, L., and Kirstetter, P.-E.: Geostatistical radar–raingauge merging: A novel method for the quantification of rain estimation accuracy, Adv. Water Resour., 71, 110–124, doi:10.1016/j.advwatres.2014.06.005, 2014.

Drobinski, P., Ducrocq, V., Alpert, P., Anagnostou, E., Béranger, K., Borga, M., Braud, I., Chanzy, A., Davolio, S., Delrieu, G., Estournel, C., Boubrahmi, N. F., Font, J., Grubisic, V., Gualdi, S., Homar, V., Ivancan-Picek, B., Kottmeier, C., Kotroni, V., Lagouvardos, K., Lionello, P., Llasat, M. C., Ludwig, W., Lutoff, C., Mariotti, A., Richard, E., Romero, R., Rotunno, R., Roussot, O., Ruin, I., Somot, S., Taupier-Letage, I., Tintore, J., Uijlenhoet, R., and Wernli, H.: HyMeX, a 10-year multidisciplinary program on the Mediterranean water cycle, B. Am. Meteor. Soc., 95, 1063–1082, doi:10.1175/BAMS-D-12-00242.1, 2013.

Duband, D., Obled, C., and Rodriguez, J. Y.: Unit hydrograph revisited: an alternate iterative approach to UH and effective precipitation identification, J. Hydrol., 150, 115–149, doi:10.1016/0022-1694(93)90158-6, 1993.

Etchevers, P., Durand, Y., Habets, F., Martin, E., and Noilhan, J.: Impact of spatial resolution on the hydrological simulation of the Durance high-Alpine catchment, France, Ann. Glaciol., 32, 87–92, 2001.

Freeze, R. A. and Harlan, R. L.: Blueprint for a physically-based, digitally-simulated hydrologic response model, J. Hydrol., 9, 237–258, doi:10.1016/0022-1694(69)90020-1, 1969.

Fu, B. P.: On the calculation of the evaporation from land surface (in Chinese), Sci. Atmos. Sin., 5, 23–31, 1981.

Gaál, L., Szolgay, J., Kohnová, S., Parajka, J., Merz, R., Viglione, A., and Blöschl, G.: Flood timescales: Understanding the interplay of climate and catchment processes through comparative hydrology, Water Resour. Res., 48, W04511, doi:10.1029/2011WR011509, 2012.

Gao, Z. Q., Liu, C. S., Gao, W., and Chang, N. B.: A coupled remote sensing and the Surface Energy Balance with Topography Algorithm (SEBTA) to estimate actual evapotranspiration over heterogeneous terrain, Hydrol. Earth Syst. Sci., 15, 119–139, doi:10.5194/hess-15-119-2011, 2011.

Garambois, P. A., Roux, H., Larnier, K., Castaings, W., and Dartus, D.: Characterization of process-oriented hydrologic model behavior with temporal sensitivity analysis for flash floods in Mediterranean catchments, Hydrol. Earth Syst. Sci., 17, 2305–2322, doi:10.5194/hess-17-2305-2013, 2013.

Gaume, E., Bain, V., Bernardara, P., Newinger, O., Barbuc, M., Bateman, A., Blaškovičová, L., Blöschl, G., Borga, M., Dumitrescu, A., Daliakopoulos, I., Garcia, J., Irimescu, A., Kohnova, S., Koutroulis, A., Marchi, L., Matreata, S., Medina, V., Preciso, E., Sempere-Torres, D., Stancalie, G., Szolgay, J., Tsanis, I., Velasco, D., and Viglione, A.: A compilation of data on European flash floods, J. Hydrol., 367, 70–78, doi:10.1016/j.jhydrol.2008.12.028, 2009.

Gottardi, F.: Estimation statistique et reanalyse des precipitations en montagne – Utilisation d'ébauches par types de temps et assimilation de donnees d'enneigement : Application aux grands massifs montagneux francais, Hydrology, Institut Polytechnique de Grenoble-INPG, French, https://tel.archives-ouvertes.fr/, 261 pp., 2009.

Gudulas, K., Voudouris, K., Soulios, G., and Dimopoulos, G.: Comparison of different methods to estimate actual evapotranspiration and hydrologic balance, Desalination Water Treat., 51, 2945–2954, doi:10.1080/19443994.2012.748443, 2013.

Gupta, H. V., Sorooshian, S., and Yapo, P. O.: Status of automatic calibration for hydrologic models: Comparison with multilevel expert calibration, J. Hydrol. Eng., 4, 135–143, 1999.

Hernández, E., Cana, L., Díaz, J., García, R., and Gimeno, L.: Mesoscale convective complexes over the western Mediterranean area during 1990–1994, Meteorl. Atmos. Phys., 68, 1–12, 1998.

Hrachowitz, M., Savenije, H. H. G., Blöschl, G., McDonnell, J. J., Sivapalan, M., Pomeroy, J. W., Arheimer, B., Blume, T., Clark, M. P., Ehret, U., Fenicia, F., Freer, J. E., Gelfan, A., Gupta, H. V., Hughes, D. A., Hut, R. W., Montanari, A., Pande, S., Tetzlaff, D., Troch, P. A., Uhlenbrook, S., Wagener, T., Winsemius, H. C., Woods, R. A., Zehe, E., and Cudennec, C.: A decade of Predictions in Ungauged Basins (PUB) – a review, Hydrol. Sci. J., 58, 1198–1255, doi:10.1080/02626667.2013.803183, 2013.

Kirchner, J. W.: Getting the right answers for the right reasons: Linking measurements, analyses, and models to advance the science of hydrology, Water Resour. Res., 42, W03S04, doi:10.1029/2005wr004362, 2006.

Kirchner, J. W.: Catchments as simple dynamical systems: Catchment characterization, rainfall-runoff modeling, and doing hydrology backward, Water Resour. Res., 45, W02429, doi:10.1029/2008WR006912, 2009.

Klemes, V.: Operational testing of hydrological simulation models, Hydrol. Sci. J., 31, 13–24, 1986.

Klemeš, V.: Conceptualization and scale in hydrology, J. Hydrol., 65, 1–23, doi:10.1016/0022-1694(83)90208-1, 1983.

Krier, R., Matgen, P., Goergen, K., Pfister, L., Hoffmann, L., Kirchner, J. W., Uhlenbrook, S., and Savenije, H. H. G.: Inferring catchment precipitation by doing hydrology backward: A test in 24 small and mesoscale catchments in Luxembourg, Water Resour. Res., 48, W10525, doi:10.1029/2011WR010657, 2012.

Lafaysse, M., Hingray, B., Etchevers, P., Martin, E., and Obled, C.: Influence of spatial discretization, underground water storage and glacier melt on a physically-based hydrological model of the Upper Durance River basin, J. Hydrol., 403, 116–129, 2011.

Lang, M., Moussay, D., Recking, A., and Naulet, R.: Hydraulic modelling of historical floods: a case study on the Ardeche river at Vallon-Pont-d'Arc, 183–189, 2002.

Le Coz, J., Hauet, A., Pierrefeu, G., Dramais, G., and Camenen, B.: Performance of image-based velocimetry (LSPIV) applied to flash-flood discharge measurements in Mediterranean rivers, J. Hydrol., 394, 42–52, doi:10.1016/j.jhydrol.2010.05.049, 2010.

Le Coz, J., Renard, B., Bonnifait, L., Branger, F., and Le Boursicaud, R.: Combining hydraulic knowledge and uncertain gaugings in the estimation of hydrometric rating curves: A Bayesian approach, J. Hydrol., 509, 573–587, doi:10.1016/j.jhydrol.2013.11.016, 2014.

Le Lay, M. and Saulnier, G. M.: Exploring the signature of climate and landscape spatial variabilities in flash flood events: Case of the 8–9 September 2002 Cévennes-Vivarais catastrophic event, Geophys. Res. Lett., 34, L13401, doi:10.1029/2007GL029746, 2007.

Manus, C., Anquetin, S., Braud, I., Vandervaere, J. P., Creutin, J. D., Viallet, P., and Gaume, E.: A modeling approach to assess the hydrological response of small mediterranean catchments to the variability of soil characteristics in a context of extreme events, Hydrol. Earth Syst. Sci., 13, 79–97, doi:10.5194/hess-13-79-2009, 2009.

McDonnell, J. J., Sivapalan, M., Vaché, K., Dunn, S., Grant, G., Haggerty, R., Hinz, C., Hooper, R., Kirchner, J., Roderick, M. L., Selker, J., and Weiler, M.: Moving beyond heterogeneity and process complexity: A new vision for watershed hydrology, Water Resour. Res., 43, W07301, doi:10.1029/2006WR005467, 2007.

Melsen, L. A., Teuling, A. J., van Berkum, S. W., Torfs, P. J. J. F., and Uijlenhoet, R.: Catchments as simple dynamical systems: A case study on methods and data requirements for parameter identification, Water Resour. Res., 50, 5577–5596, doi:10.1002/2013WR014720, 2014.

Molinié, G., Ceresetti, D., Anquetin, S., Creutin, J. D., and Boudevillain, B.: Rainfall Regime of a Mountainous Mediterranean Region: Statistical Analysis at Short Time Steps, J. Appl. Meteorol. Climatol., 51, 429–448, doi:10.1175/2011JAMC2691.1, 2011.

Moriasi, D. N., Arnold, J. G., Van Liew, M. W., Bingner, R. L., Harmel, R. D., and Veith, T. L.: Model evaluation guidelines for systematic quantification of accuracy in watershed simulations, Trans. ASABE, 50, 885–900, 2007.

Nash, J. E. and Sutcliffe, J. V.: River flow forecasting through conceptual models part I – A discussion of principles, J. Hydrol., 10, 282–290, 1970.

Naulet, R., Lang, M., Ouarda, T. B. M. J., Coeur, D., Bobée, B., Recking, A., and Moussay, D.: Flood frequency analysis on the Ardèche river using French documentary sources from the last two centuries, J. Hydrol., 313, 58–78, 2005.

Pike, J. G.: The estimation of annual run-off from meteorological data in a tropical climate, J. Hydrol., 2, 116–123, doi:10.1016/0022-1694(64)90022-8, 1964.

Quintana-Seguí, P., Le Moigne, P., Durand, Y., Martin, E., Habets, F., Baillon, M., Canellas, C., Franchisteguy, L., and Morel, S.: Analysis of near-surface atmospheric variables: Validation of the SAFRAN analysis over France, J. Appl. Meteorol. Climatol., 47, 92–107, 2008.

Samaniego, L., Kumar, R., and Attinger, S.: Multiscale parameter regionalization of a grid-based hydrologic model at the mesoscale, Water Resour. Res., 46, W05523, doi:10.1029/2008WR007327, 2010.

Saulnier, G. M. and Le Lay, M.: Sensitivity of flash-flood simulations on the volume, the intensity, and the localization of rainfall in the Cévennes-Vivarais region (France), Water Resour. Res., 45, W10425, doi:10.1029/2008WR006906, 2009.

Schreiber, P.: Über die Beziehungen zwischen dem Niederschlag und der Wasserführung der Flüsse in Mitteleuropa, Zeitschr. Meteorol., 21, 441–452, 1904.

Seiler, C. and Moene, A. F.: Estimating Actual Evapotranspiration from Satellite and Meteorological Data in Central Bolivia, Earth Interact., 15, 1–24, doi:10.1175/2010EI332.1, 2010.

Sempere-Torres, D., Rodriguez-Hernandez, J. Y., and Obled, C.: Using the DPFT approach to improve flash flood forecasting models, Nat. Hazards, 5, 17–41, 1992.

Sheffer, N. A., Enzel, Y., and Benito, G.: Paleofloods in southern France-the Ardeche River, PHEFRA workshop, Barcelona, 25–31, 2002.

Sivapalan, M.: Process complexity at hillslope scale, process simplicity at the watershed scale: is there a connection?, Hydrological Processes, 17, 1037–1041, doi:10.1002/hyp.5109, 2003a.

Sivapalan, M.: Prediction in ungauged basins: a grand challenge for theoretical hydrology, Hydrol. Proc., 17, 3163–3170, doi:10.1002/hyp.5155, 2003b.

Sivapalan, M.: Pattern, Process and Function: Elements of a Unified Theory of Hydrology at the Catchment Scale, in: Encyclopedia of Hydrological Sciences, John Wiley & Sons, Ltd, Chichester, UK, 193–219, doi:10.1002/0470848944.hsa012, 2006.

Tarboton, D. G., Schreuders, K. A. T., Watson, D. W., and Baker, M. E.: Generalized terrain-based flow analysis of digital elevation models, 18th World IMACS Congress and MODSIM09 International Congress on Modelling and Simulation, 2000–2006, 2009.

Tekleab, S., Uhlenbrook, S., Mohamed, Y., Savenije, H. H. G., Temesgen, M., and Wenninger, J.: Water balance modeling of Upper Blue Nile catchments using a top-down approach, Hydrol. Earth Syst. Sci., 15, 2179–2193, doi:10.5194/hess-15-2179-2011, 2011.

Teuling, A. J., Lehner, I., Kirchner, J. W., and Seneviratne, S. I.: Catchments as simple dynamical systems: Experience from a Swiss prealpine catchment, Water Resour. Res., 46, W10502, doi:10.1029/2009WR008777, 2010.

Thierion, C., Longuevergne, L., Habets, F., Ledoux, E., Ackerer, P., Majdalani, S., Leblois, E., Lecluse, S., Martin, E., Queguiner, S., and Viennot, P.: Assessing the water balance of the Upper Rhine Graben hydrosystem, J. Hydrol., 424–425, 68–83, doi:10.1016/j.jhydrol.2011.12.028, 2012.

Thornthwaite, C. and Mather, J.: The water balance, Climatology, VIII, New Jersey, NY, 1–37, 1955.

Tramblay Y., Bouvier C., Crespy A., and Marchandise A.: Improvement of flash flood modelling using spatial patterns of rainfall: a case study in south of France. Global Change: Facing Risks and Threats to Water Resources Proceedings of the Sixth World FRIEND Conference, Fez, Morocco, October 2010, IAHS Publ. 340, 172–178, http://y.tramblay.free.fr/doc/Tramblay-redbook.340.pdf, 2010.

Turc, L.: Nouvelles formules pour le bilan d'eau en fonction des valeurs moyennes annuelles de précipitations et de la température, Comptes Rendus de l'Académie des Sciences, Paris, 233, 633–635, 1951.

Uhlenbrook, S., Seibert, J. A. N., Leibundgut, C., and Rodhe, A.: Prediction uncertainty of conceptual rainfall-runoff models caused by problems in identifying model parameters and structure, Hydrol. Sci. J., 44, 779–797, doi:10.1080/02626669909492273, 1999.

Vannier, O.: Apport de la modélisation hydrologique régionale à la compréhension des processus de crue en zone méditerranéenne, Thèse de l'Ecole doctorale Terre, Univers, Environnement, University of Grenoble, Grenoble, France, 22 November 2013, 274 pp., 2013.

Vannier, O., Braud, I., and Anquetin, S.: Regional estimation of catchment-scale soil properties by means of streamflow recession analysis for use in distributed hydrological models, Hydrol. Proc., 28, 6276–6291, doi:10.1002/hyp.10101, 2014.

Vidal, J. P., Martin, E., Franchistéguy, L., Baillon, M., and Soubeyroux, J. M.: A 50-year high-resolution atmospheric reanalysis over France with the Safran system, Int. J. Climatol., 30, 1627–1644, 2010.

Yan, Z., Gottschalk, L., Leblois, E., and Xia, J.: Joint mapping of water balance components in a large Chinese basin, J. Hydrol., 450–451, 59–69, doi:10.1016/j.jhydrol.2012.05.030, 2012.

Wittenberg, H. and Sivapalan, M.: Watershed groundwater balance estimation using streamflow recession analysis and baseflow separation, J. Hydrol., 219, 20–33, doi:10.1016/s0022-1694(99)00040-2, 1999.

Zehe, E., Lee, H., and Sivapalan, M.: Dynamical process upscaling for deriving catchment scale state variables and constitutive relations for meso-scale process models, Hydrol. Earth Syst. Sci., 10, 981–996, doi:10.5194/hess-10-981-2006, 2006.

Zhang, L., Hickel, K., Dawes, W. R., Chiew, F. H. S., Western, A. W., and Briggs, P. R.: A rational function approach for estimating mean annual evapotranspiration, Water Resour. Res., 40, W02502, doi:10.1029/2003WR002710, 2004.

Zhang, L., Potter, N., Hickel, K., Zhang, Y., and Shao, Q.: Water balance modeling over variable time scales based on the Budyko framework – Model development and testing, J. Hydrol., 360, 117–131, 2008.